6

NAVAL POSTGRADUATE SCHOOL
Monterey, California

SYNOPTIC CLASSIFICATION AND HORIZONTAL
HOMOGENEITY OF THE REFRACTIVE INDEX STRUCTURE
FUNCTION PARAMETER IN THE SURFACE LAYER

P. Jones Boyle and K. L. Davidson

February 1984

Technical Report: October 1981 - October 1982

Approved for public release; distribution unlimited.
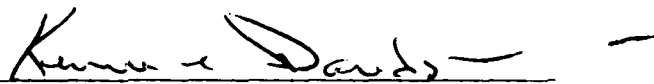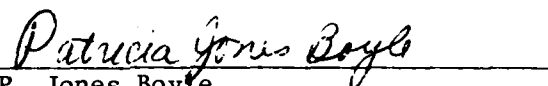
NAVAL POSTGRADUATE SCHOOL
Monterey, California 93943

Commodore R. H. Shumaker   Dean D. A. Schrady
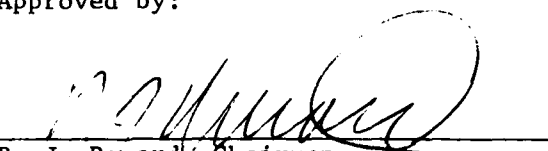Superintendent   Provost
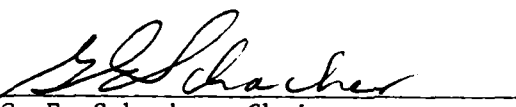

The work reported herein has been supported by NEPRF. Reproduction
of all or part of this report is authorized.

K. L. Davidson
Professor of Meteorology

P. Jones Boyle
Meteorologist

Approved by:

R. J. Renard, Chairman   G. E. Schacher, Chairman
Department of Meteorology   Department of Physics

Released by:

J. N. Dyer
Dean of Science and Engineering

REPORT DOCUMENTATION PAGE		READ INSTRUCTIONS BEFORE COMPLETING FORM
I. REPORT NUMBER NPS-63-84-001	**2. GOVT ACCESSION NO.** AD-A140925	**3. RECIPIENT'S CATALOG NUMBER**
4. TITLE (and Subtitle) Synoptic Classification and Horizontal Homogeneity of the Refractive Index Structure Function Parameter in the Surface Layer		**5. TYPE OF REPORT & PERIOD COVERED** Technical Report October 1981 – October 1982
		6. PERFORMING ORG. REPORT NUMBER
7. AUTHOR(s) P. Jones Boyle and K. L. Davidson		**8. CONTRACT OR GRANT NUMBER(s)**
9. PERFORMING ORGANIZATION NAME AND ADDRESS Naval Postgraduate School Monterey, California 93943		**10. PROGRAM ELEMENT, PROJECT, TASK AREA & WORK UNIT NUMBERS** N6685684WR82063
11. CONTROLLING OFFICE NAME AND ADDRESS Naval Environmental Prediction Research Facility Monterey, California 93943		**12. REPORT DATE** February 1984
		13. NUMBER OF PAGES 66
14. MONITORING AGENCY NAME & ADDRESS(If different from Controlling Office)		**15. SECURITY CLASS. (of this report)** Unclassified
		15a. DECLASSIFICATION/DOWNGRADING SCHEDULE

16. DISTRIBUTION STATEMENT (of this Report)

Approved for public release; distribution unlimited.

17. DISTRIBUTION STATEMENT (of the abstract entered in Block 20, If different from Report)

18. SUPPLEMENTARY NOTES

19. KEY WORDS (Continue on reverse side if necessary and identify by block number)

Optical Turbulence, Optical Turbulence Synoptic Classification
Optical Turbulence Horizontal Homogeneity
Surface Layer C_n^2
REG Classification of Optical Turbulence

20. ABSTRACT (Continue on reverse side if necessary and identify by block number)

This is a two part report. The first part describes an investigation of the feasibility of using the synoptic scale classification scheme described in the Refractive Effects Guidebook (REG) to predict the level of optical turbulence in the surface layer as measured by C_n^2, the refractive index structure function parameter. Data were examined from nine experiments which took place in the north Pacific and north Atlantic. The measurement experiments spanned five years and included all four seasons. The REG appears to be

DD FORM 1473 EDITION OF 1 NOV 65 IS OBSOLETE
1 JAN 73
S/N 0102-014-6601

useful in a limited way in predicting ranges of C_n^2 in the surface layer. Inclusion of local factors would increase predictability. The second part deals with horizontal homogeneity of the surface layer C_n^2 as measured during the JASIN experiment in the North Atlantic in 1978. Periods of homogeneity lasting between one and two days were encountered along 200 km sectors and for up to nine hours over the entire JASIN experimental area.

ACKNOWLEDGEMENTS

TABLE OF CONTENTS

LIST OF TABLES

LIST OF FIGURES

1. INTRODUCTION

This report presents results from the application of a classification scheme designed for synoptic scale atmospheric refractive conditions which affect radar propagation to the surface layer refractive index structure function parameter, C_n^2. The classification scheme is described in the Refractive Effects Guidebook (REG) (Rosenthal, 1976). It is referred to in this report as the REG classification. Also described herein are the results of an analysis of the horizontal homogeneity of C_n^2 from data taken in the North Atlantic during the JASIN study in 1978.

The REG classification was applied to C_n^2 by McPherson (1981). This report includes a re-evaluation of most of the data sets used by McPherson, and further includes data from two cruises in the Pacific. One of the cruises took place in the summer, (MABLE), the other in early winter (STREX). Additional data from JASIN were also included in this analysis. C_n^2 values were estimated by the bulk method and examined according to REG category for value ranges, diurnal variation and probability distributions. The bulk method relates C_n^2 to wind, temperature and humidity through the structure functions C_T^2, C_Q^2 and C_{TQ}.

Horizontal homogeneity of C_n^2 was examined on the basis of the JASIN data set in which concurrent data were available from three ships in the 'JASIN triangle'. The bulk method was used to estimate C_n^2 at each corner of the triangle, and horizontal homogeneity was determined within the accuracy limits of the measurement errors and the bulk parameterization.

2. SYNOPTIC CLASSIFICATION AND C_N^2

2.1 REG CLASSIFICATION SYSTEM

The REG was designed to relate atmospheric electro-magnetic (EM) refractive conditions to synoptic weather patterns. Since optical turbulence depends on the same parameters as EM propagation anomalies (near-surface stability, height and strength of inversion), synoptic regimes associated with radar refractive conditions would be expected to be associated with optical turbulence conditions. Various optical turbulence condtions would be reflected in the values of C_n^2 encountered under different REG synoptic categories.

In this study, REG categories were assigned to each day of the experiments on the basis of surface weather maps. The terms REG category and REG regime will be used interchangeably throughout this report. The REG diagram for the appropriate ocean and season was used to determine which REG category applied to the region in which the experimental data were collected. The entire data set encompssed seven of the eleven REG regimes: B, C,D,E,F,J and K. In Table 1 are presented the REG ducting conditions, the type of temperature inversion and air mass for each of these profile types.

Figures 1a-1h, reproduced from the REG, are synoptic charts for the North Pacific and North Atlantic, superimposed with REG category regimes. They represent typical synoptic patterns found in each ocean during all four seasons of the year. The experiments in this study spanned all seasons and occurred in both the North Atlantic and North Pacific.

The REG is based on air mass properties and inversion heights. If it can be used to delineate different optical turbulence regimes, it would be useful in predicting periods of high turbulence in which the performance of electro-optical systems would be ser iusly degraded.

TABLE 1
REG Profile Conditions

Profile	Ducting	Temperature Inversion	Air Mass
B	strong, surface based, top near 2000 ft.	Moderate, elevated	Subtropical
C	very low, based at or just above surface, top near 600 ft.	Strong, surface based	Polar
D	sharp, elevated, based near 1500 ft., top at 2300 ft.	Moderate, elevated	Modified Polar
E	sharp, deep, elevated, base near 4000 ft., top at 5700 ft.	Strong elevated	Tropical
F	very sharp, high, elevated, base near 9200 ft., top near 10300 ft.	---------	Modified Tropical
J	multiple ducts and sub-refractive layers up to 8000 ft.	---------	Modified Tropical
K	no significant refractive layers	standard, well-mixed atmosphere	Temperature

North Pacific, Winter
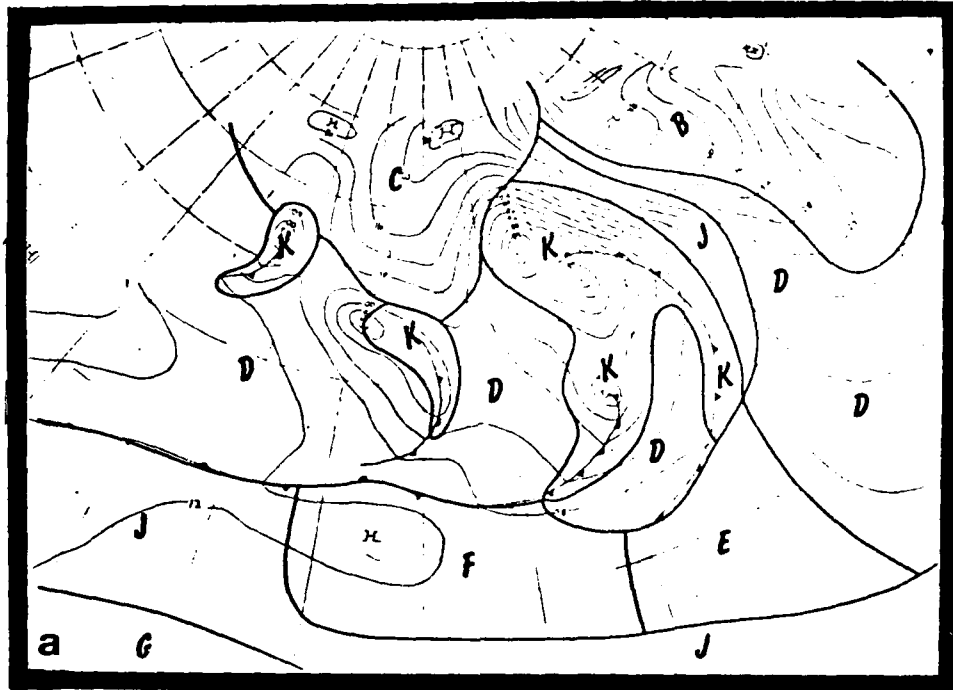
North Pacific,Spring
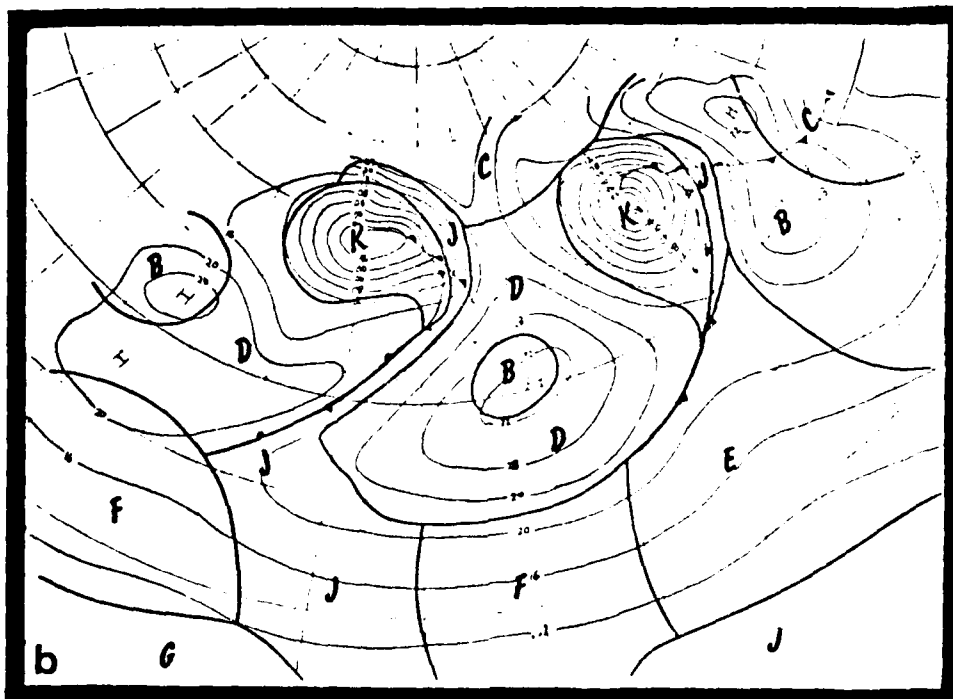
Figure 1. REG profile regions and typical synoptic patterns for the North Atlantic and North Pacific.

North Pacific, Summer
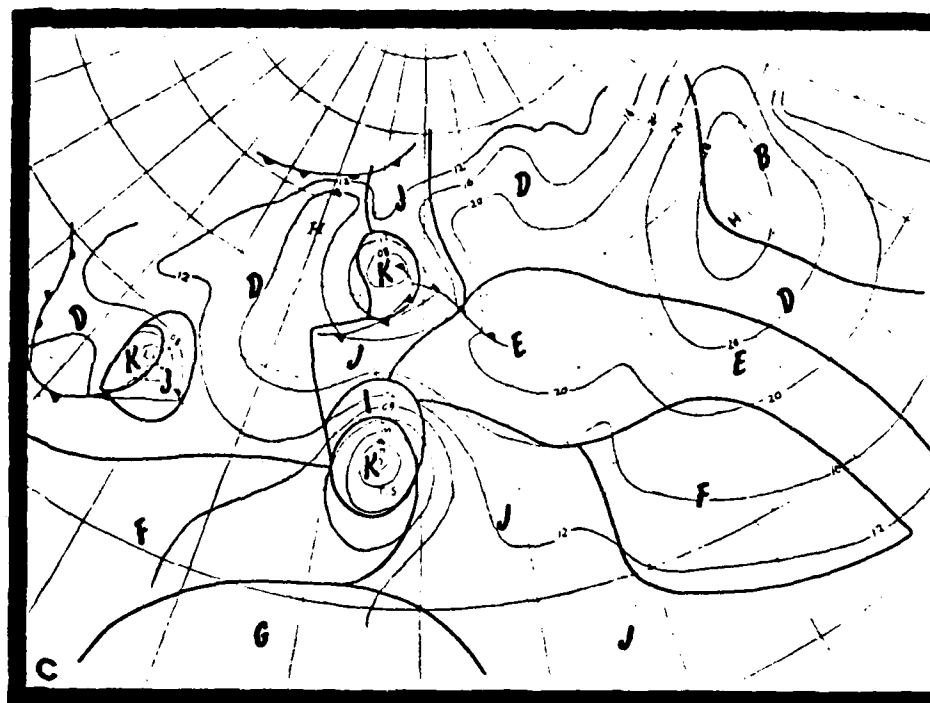
North Pacific, Fall
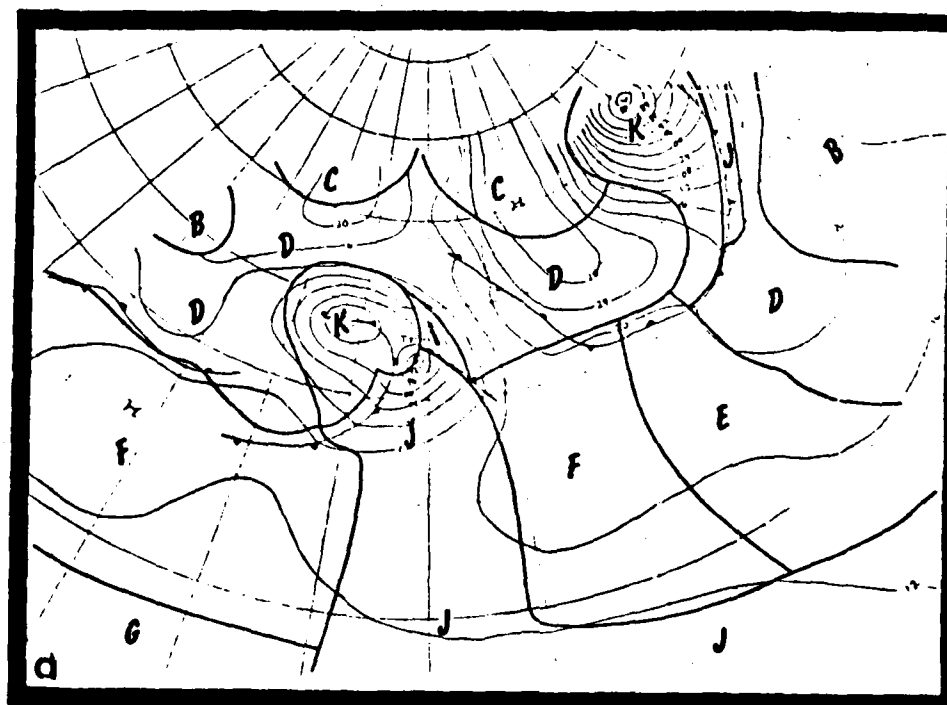
North Atlantic, Winter
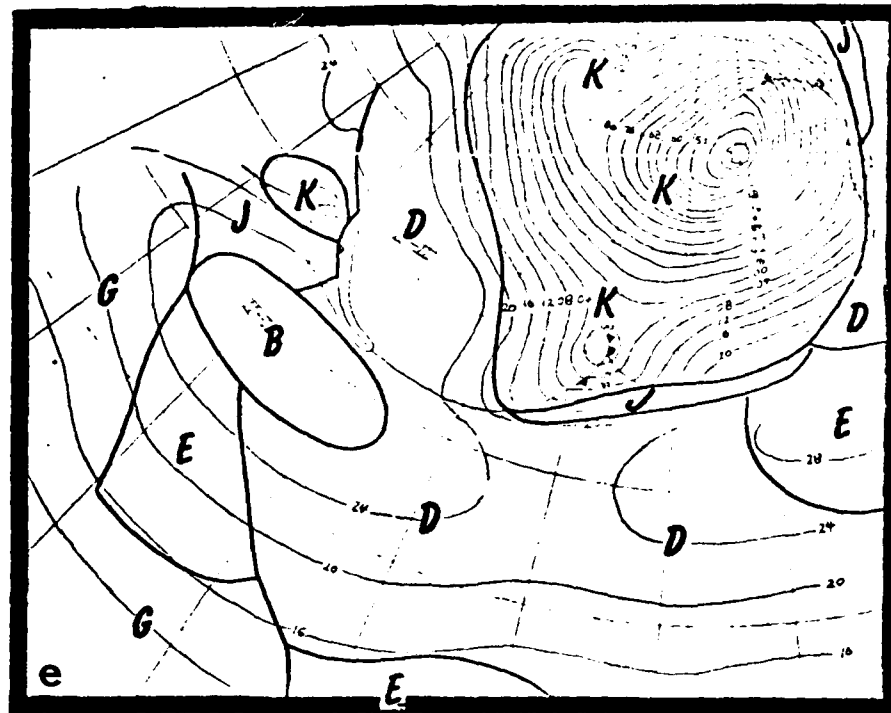
North Atlantic, Spring
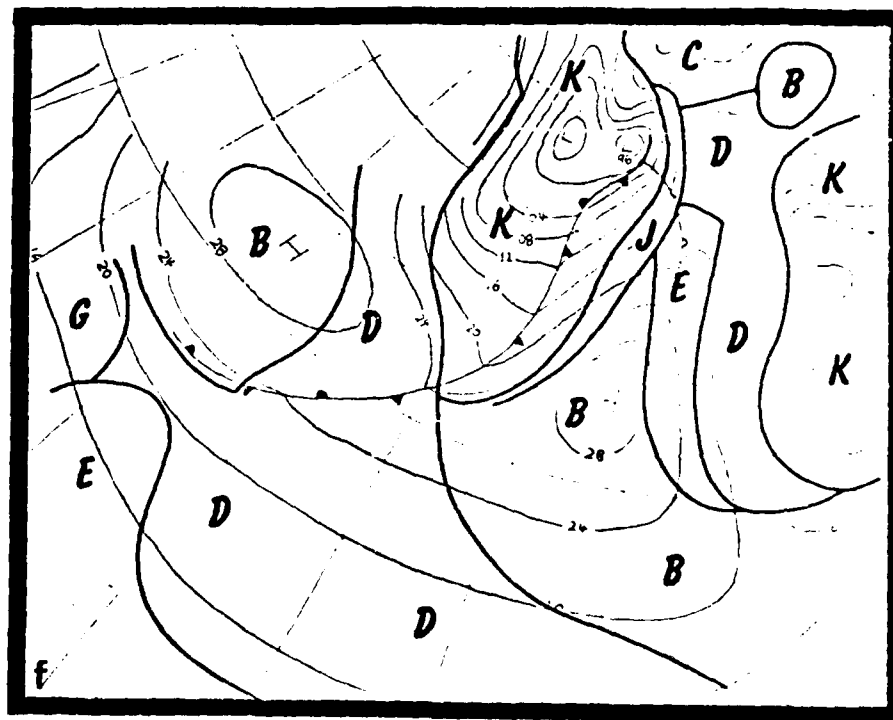
North Atlantic, Summer
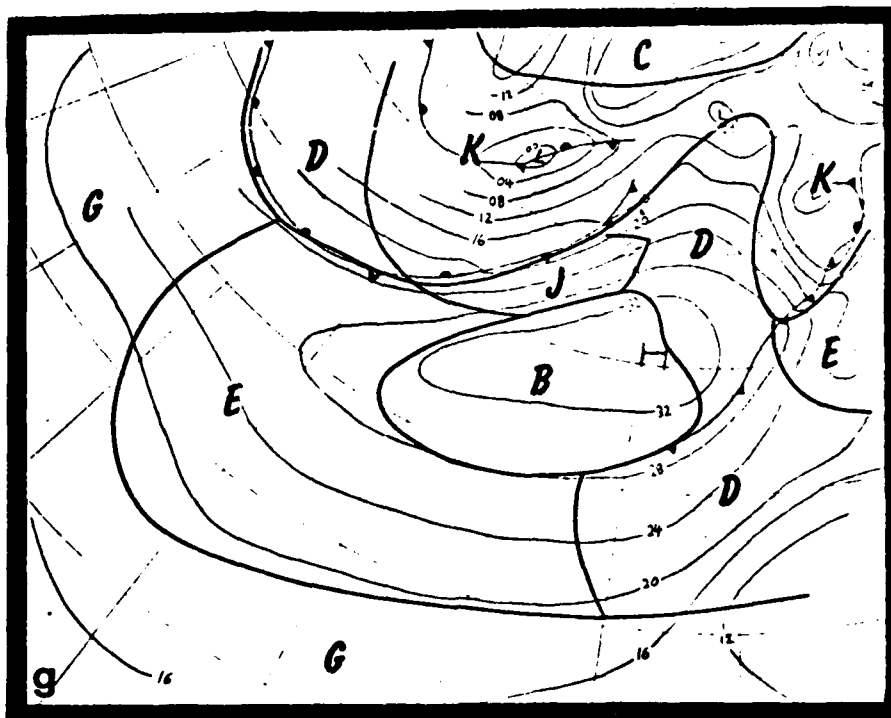
North Atlantic, Fall
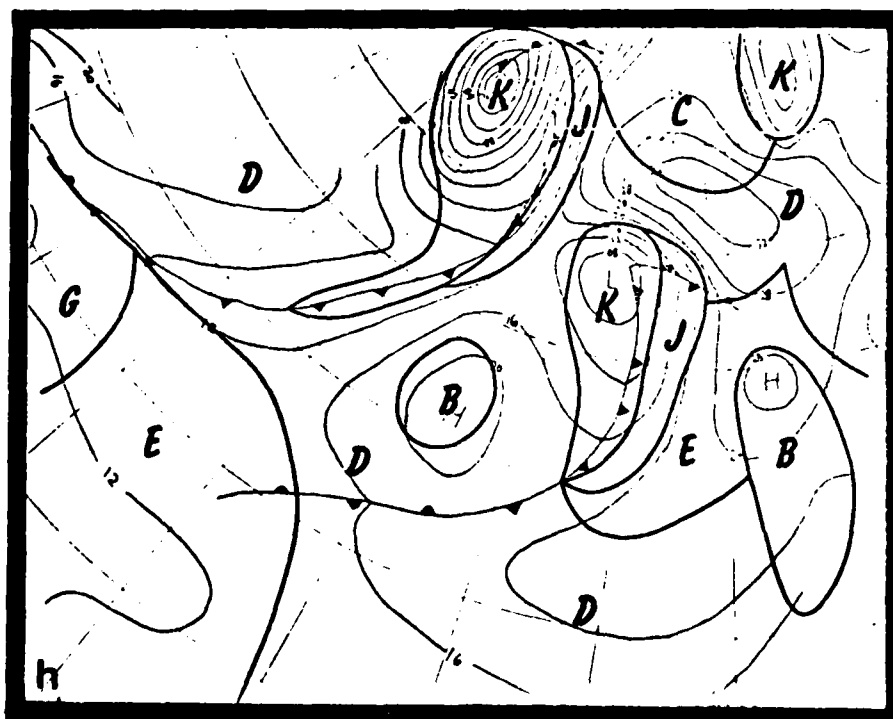
2.2   METEOROLOGICAL DATA

2.2.1 Experiments

The data came from nine experiments conducted in both the Atlantic and Pacific under widely varying meteorological conditions. In Table 2 the experiments in which the data were collected are listed, along with the specific ships involved, location, dates, and the number of days in each experiment with particular REG categories. Appendix A contains specific information regarding REG categories and individual experiment dates.

TABLE 2

Experiment Summary

Experiment	Ship	Location	Dates	REG profiles			
KANE	USNS Kane	mid-Atlantic	Mar 1978	14B,	1J		
MAGAT	R/V Acania	Monterey Bay	Apr-May 1980	6D,	6E		
CEWCOM-78	R/V Acania	east Pacific	May 1978	2D,	3E,	5F	
CTQ	R/V Acania	Monterey Bay	Jun 1979	6B,	1D		
ARB	R/V Acania	east Pacific	Jul 1977	5B,	3D		
MABLE	R/V Acania	east Pacific	Aug 1978	7B,	1D,	8E,	2J
JASIN	J. MURRAY G. ENDURER HECLA METEOR CHALLENGER	no. Atlantic	Jul-Sep 1978	1B,	31D,	5J,	20K
CEWCOM-76	R/V Acania	east Pacific	Sep-Oct 1976	3D,	7E,	5F,	3K
STREX	Oceanographer	Gulf of Alaska	Nov-Dec 1980	2B,	4C,	8D,	1J, 17K

2.2.2 Data Acquisition

Measurements of wind speed, air and sea temperature and humidity were required to calculate $C_n{}^2$. Surface layer $C_n{}^2$ values are very insensitive to pressure, so a value of 1000 mb was used for all experiments except JASIN, for which pressure measurements were available. Instrumentation varied from ship to ship, but most of the data examined here were obtained by the Environmental Physics Group (EPG) of the Naval Postgraduate School (NPS). Several reports exist which discuss the instruments used on particular NPS experiments.

Schacher et al (1980) describes the NPS instrumentation used on the R/V Acania, the NOAA ship Oceanographer, and HMS Challenger. Fairall et al (1978) describes the instrumentation used on the USNS KANE, and Spiel (1981) gives further information regarding NPS instrumentation and data gathered on the Oceanographer. A brief summary of NPS measurement instruments and accuracies is provided here.

Wind speed was measured with cup anemometers; the accuracy of the various anemometers used ranged from 1% to 5%. Air temperature measurements were made with either a quartz oscillator thermometer or Rosemount platinum resistors. The accuracy of the quartz oscillator thermometer is 0.01 C; the Rosemount system has an accuracy of 0.2 C. Sea-surface temperature was also measured with a platinum resistor with a 0.2 C accuracy. Humidity was determined either by measuring relative humidity with a LiCl cell, having a 3% accuracy, or by measuring dewpoint temperature with a platinum resistor system accurate to 0.22 C.

The JASIN shipboard data from the METEOR, ENDURER, HECLA and MURRAY included hourly observations of wind speed, air, wet bulb and sea-surface (bucket) temperatures, and pressure. The accuracy of the temperatures was 0.2 C, of pressure, 1 mb and of wind speed, 1 kt (.515 m s^{-1}). Documentation exists on the JASIN experiment and the reader is referred to the Royal Society (1978) and Royal Society (1979) reports for further information. Inter-platform measurement comparisons between the four ships were made by Macklin and Guymer (1980). Their corrections to the raw data were applied to the measurements used in this study.

Figure 2 illustrates the instrumentation arrangements used aboard the ships. Table 3 presents values of accuracy assumed for the entire data set.

-15-
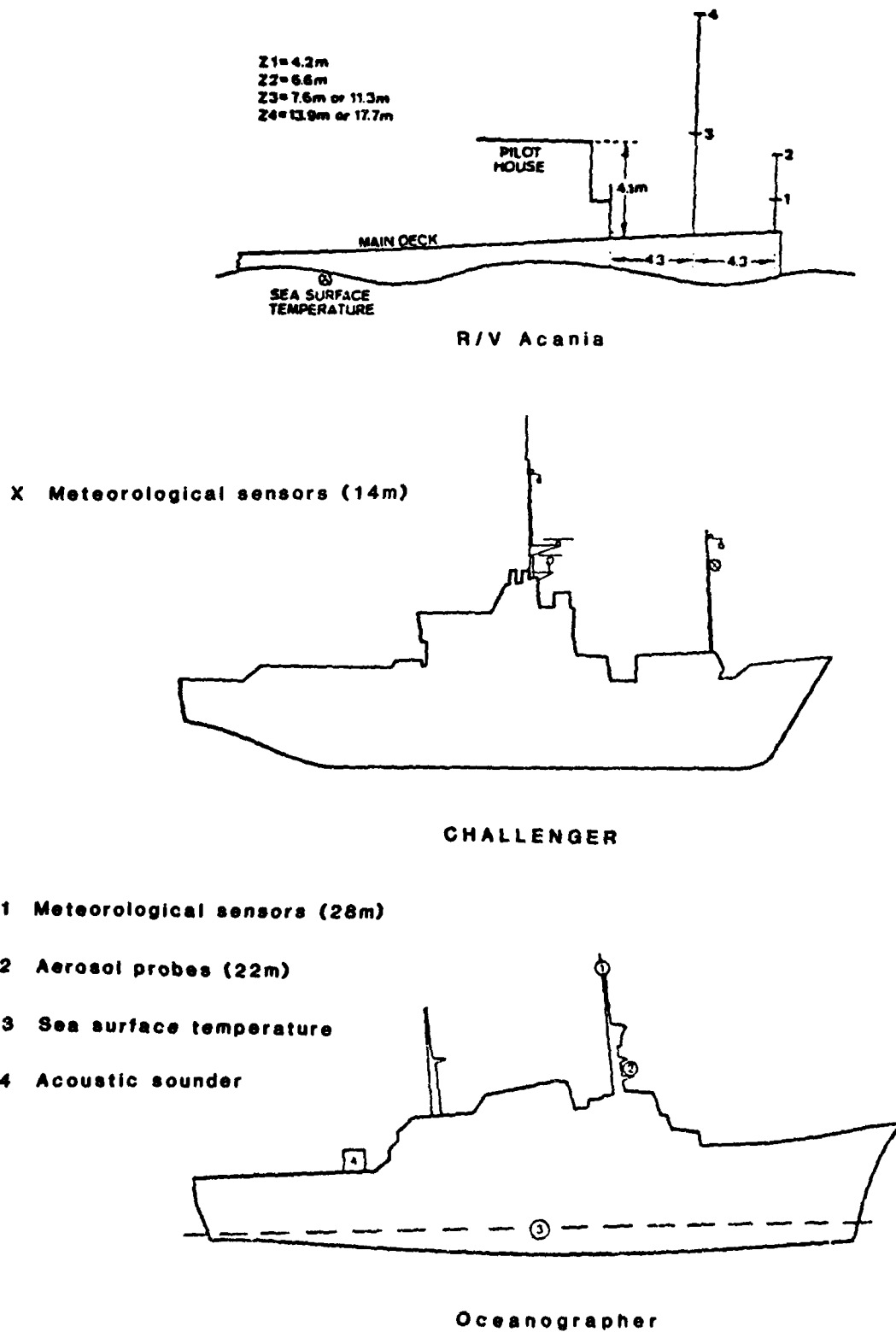
Figure 2. Schematics of ships used in meteorological experiments.

R.V. METEOR

H.M.S. HECLA

R.R.S. JOHN MURRAY

M.V. GARDLINE ENDURER
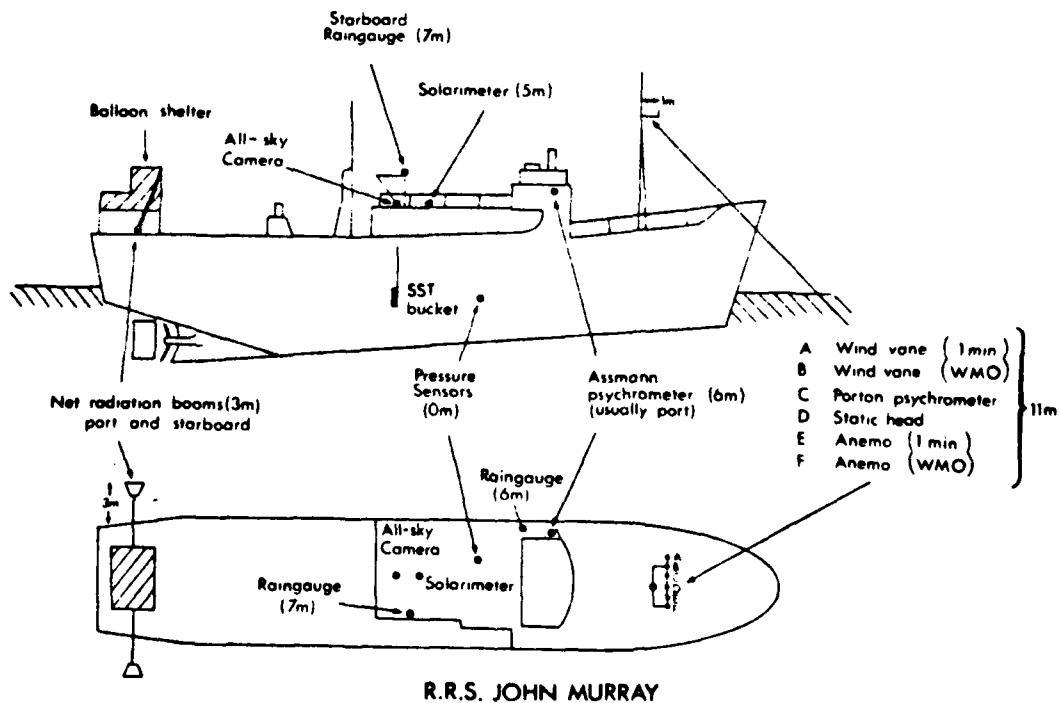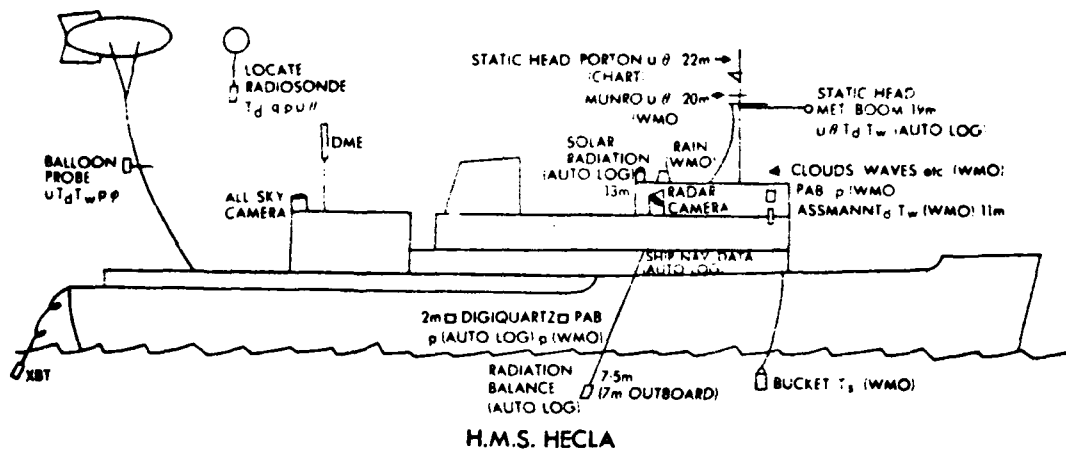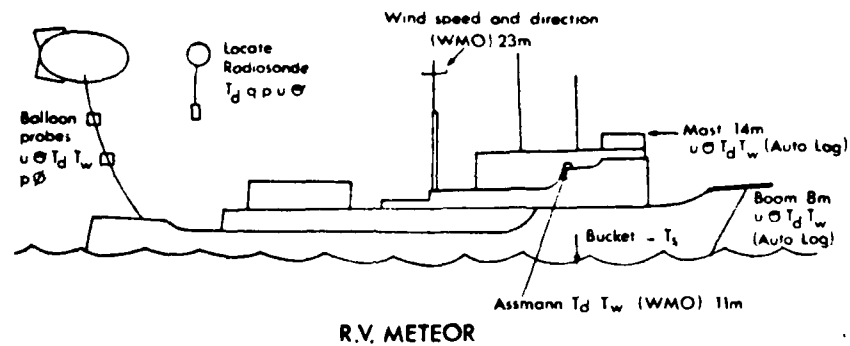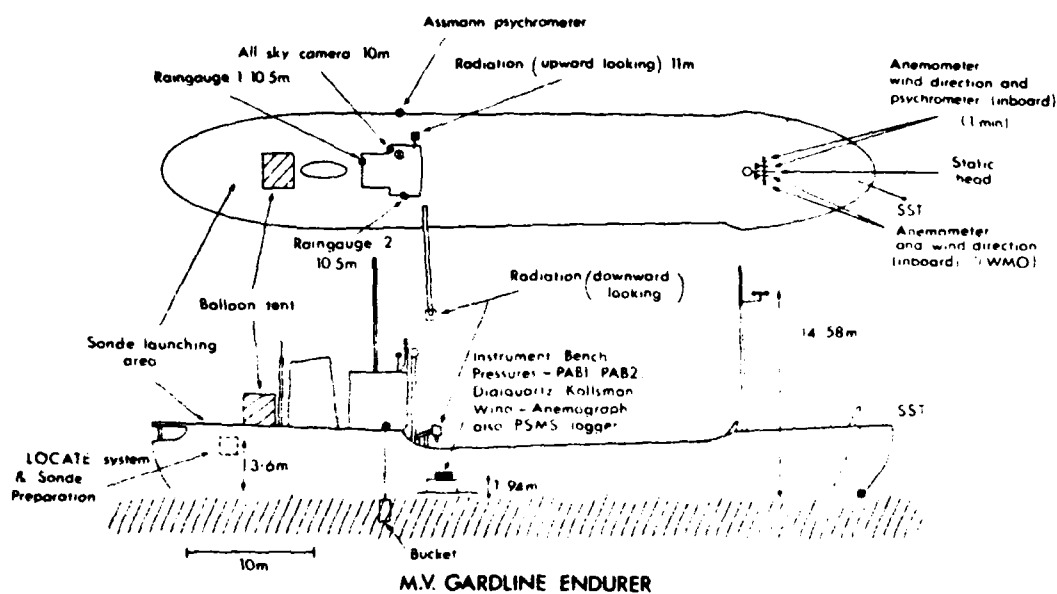
Z1 = 2.8m
Z2 = 9.1m
Z3 = 18.6m
Z4 = 24.7m

USNS Kane
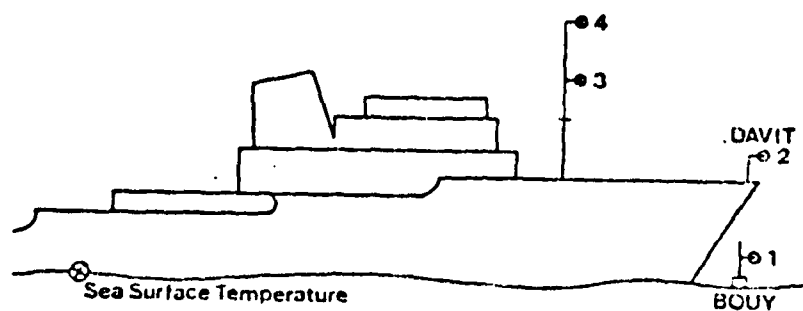
TABLE 3

Accuracy of Meteorological Parameters

Parameter	Accuracy
wind speed	5%
air temperature	0.22 C
sea surface temperature	0.22 C
relative humidity	3%
pressure	1 mb

2.3 C_n^2 CALCULATIONS

With the exception of JASIN data from the METEOR, HECLA, ENDURER and MURRAY, data were available in the form of 30 minute averages. C_n^2 was calculated for each observation period using the bulk method. The midpoint of the observation period was rounded to the nearest hour; all sets of data occurring within the same hour were averaged, giving hourly averaged values of C_n^2, air and sea temperature, stability (Z/L), wind speed and relative humidity. The JASIN data from the four ships mentioned above consisted of hourly values available every three hours; it required no further averaging.

2.3.1 Bulk Aerodynamic Method

The bulk aerodynamic method of estimating C_n^2 relates the optical refractive index structure function parameter to temperature and humidity through their structure function parameters (C_T^2 and C_Q^2, respectively) and through C_{TQ}, the temperature-humidity cospectral structure function parameter.

This is expressed in Eqn. (1) (Friehe, 1977):

$$C_n^2 = (79 \times 10^{-6} \ P/T^2)^2 \ (C_T^2 + .113 \ C_{TQ} + 3.2 \times 10^{-3} \ C_Q^2) \tag{1}$$

Fairall (1980) provides a full discussion of the bulk method used for estimating C_n^2. The symbols used in all equations are explained in Table 4. C_T^2, C_Q^2 and C_{TQ} can be calculated using Monin-Obukhov similarity parameters

-19-

T_* (potential temperature scaling parameter) and q_* (water vapor mixing ratio scaling parameter) as follows:

$$C_T^2 = T_*^2 \; Z^{-2/3} \; f(\xi) \tag{2a}$$

$$C_Q^2 = Q_*^2 \; Z^{-2/3} \; Af(\xi) \tag{2b}$$

$$C_{TQ} = r_{TQ} \; T_* Q_* \; Z^{-2/3} \; Af(\xi) \tag{2c}$$

where $\quad Q_* = 1.3 \; q_*$

$\qquad \xi = Z/L$

$\qquad f(\xi) = 4.9(1-7 \; \xi)^{2/3} \qquad$ if $\xi < 0$

$\qquad \quad = 4.9(1+2.4 \; \xi^{2/3}) \qquad$ if $\xi \geq 0$

In this study the similarity parameter equations were modified in unstable cases in which $\xi < -1$ using local-free convection scaling (Wyngaard, 1973). The modifications are discussed in section 2.3.2. The Monin-Obukhov length scale L, is defined as:

$$\frac{1}{L} = \frac{kg}{T} \frac{(T_* + 6.1 \times 10^{-4} \; Tq_*)}{U_*^2} \tag{3}$$

To estimate C_n^2 using Eqn (1) all that remains to be determined are T_*, q_* and the friction velocity, U_*. These scaling parameters may be related to the difference between the value of the bulk meteorological quantity at a reference height Z' and the surface through the profile equations (Businger, 1973):

$$u_* = kU(\ln(Z'/Z_o) - \psi_1(\xi'))^{-1} \tag{4a}$$

$$T_* = (T-T_o) \; \alpha_T k(\ln(Z'/Z_{oT}) - \psi_2(\xi'))^{-1} \tag{4b}$$

$$q_* = (q-q_o) \; \alpha_T k(\ln(Z'/Z_{oT}) - \psi_2(\xi'))^{-1} \tag{4c}$$

where the subscript o refers to surface values.

The velocity and temperature profile functions are defined as Businger, 1973):

$$\psi_1(\xi') = 2 \ln[(1+x)/2] + \ln[(1+x^2)/2] - 2 \tan^{-1}(x) + \pi/2$$

$$x = (1 - 15 \xi')^{1/4} \qquad \text{if } \xi' < 0$$

$$\psi_1(\xi') = -4.7 \xi' \qquad \text{if } \xi' \geq 0$$

$$\psi_2(\xi') = 2 \ln[(1+x)/2]$$

$$x = (1 - 9 \xi')^{1/2} \qquad \text{if } \xi' < 0$$

$$\psi^2(\xi') = -6.5 \xi' \qquad \text{if } \xi' \geq 0$$

The scaling parameters may also be expressed in terms of stability dependent drag coefficients:

$$U_* = c_D^{1/2} u \qquad\qquad (5a)$$

$$T_* = c_T^{1/2}(T-T_o) \qquad\qquad (5b)$$

$$q_* = c_T^{1/2}(q-q_o) \qquad\qquad (5c)$$

where the drag coefficients are:

$$c_D^{1/2} = \frac{k/\ln(Z'/Z_o)}{1-(\ln(Z'/Z_o))^{-1} \psi_1(\xi')}$$

$$c_T^{1/2} = \frac{\alpha_T k/\ln(Z'/Z_{oT})}{1-(\ln(Z'/Z_{oT}))^{-1} \psi_2(\xi')}$$

It is assumed that the water vapor dependencies can be treated with the same coefficients as the temperature, i.e. Z_{oT} and c_T are used for q as well as T.

For all cases except a portion of the JASIN data, values of U_* and T_* (calculated by the bulk method) and ξ (with $Z = 10$) were readily available. It was necessary to calculate only q_*. This was done by multiplying both sides of Eqn (3) by Z and solving for q_*:

$$q_* = \frac{(U_*^2 \, \xi T)(Zkg) - T_*}{6.1 \times 10^{-4} \, T} \qquad (6)$$

Data available for most of the JASIN ships included hourly measurements of wind speed, air temperature, wet bulb temperature and relative humidity at the instrument height, sea-surface temperature and surface pressure. From these, Z/L was calculated from the bulk formulas using an iterative procedure (Fairall, 1980), during which wind speed, temperature, and/or mixing ratio (depending on the ship) were scaled down from instrument height to 10 meters using the methods outlined in section 2.3.3. The CHALLENGER data were in the same format as that from all of the other experiments.

TABLE 4

Symbol Definitions

---

p $\quad$ = pressure (mb)

T $\quad$ = temperature (K)

Q_* = 1.3 q_* (q_* in gkg^{-1}, Q_* in gm^{-3})

Z $\quad$ = measurement height above the surface (m)

Z' = reference height above the surface (m)

Z_o = roughness length for velocity profile

Z_{oT} = 2×10^{-5} = roughness length for temperature profile (Fairall, 1980)

L $\quad$ = Monin-Obukhov length scale (m)

ξ $\quad$ = Z/L

ξ' = Z'/L

A $\quad$ = 0.8 (Fairall et al., 1980)

r_{TQ} = temperature-humidity correlation parameter

$\quad$ = 0.8 under unstable conditions, not well known under stable conditions (Fairall et al., 1980)

k $\quad$ = 0.35 = von Karman's constant

g $\quad$ = 9.8 m s^{-2} = acceleration due to gravity

q $\quad$ = mixing ratio (gkg^{-1})

U $\quad$ = 10 m wind speed (m s^{-1})

α_T = 1.35 = ratio of heat transfer to momentum transfer at Z=0 (Businger et al., 1971)

2.3.2 Free Convection Scaling

Wyngaard (1973) discussed scaling in the asymptotic cases on both the moderate stable side (z-less stratification) and the moderate unstable (free convection) condition. Since most of the data used in this study involved unstable regimes (see Appendix B), we will not discuss z-less stratification.

Under free convection conditions the scaling parameters U_*, T_* and Q_* are replaced by u_f, T_f and Q_f. Expressions for u_f, T_f and Q_f are:

$$U_f = (ZT_{fv}g/T)^{1/2} \qquad (7a)$$

$$T_f = T_*U_*/U_f \qquad (7b)$$

$$Q_f = Q_*U_*/U_f \qquad (7c)$$

where

$$T_{fv} = (T_v Q_o^2/gZ)^{1/3}$$

$$Q_o = \overline{w'\theta'} = -T_{*v}U_*$$

$$T_{*v} = (\theta_{vz} - \theta_{vo}) C_\theta(\xi)$$

$$C\theta(\xi) = \alpha_T k(\ln(Z/Z_{oT}) - \psi_2(\xi))^{-1}$$

The equations for the structure function parameters are:

$$C_T^2 = T_f^2 Z^{-2/3} \ 2.7 \qquad (8a)$$

$$C_Q^2 = Q_f^2 Z^{-2/3} \ 2.7A \qquad (8b)$$

$$C_{TQ} = T_f Q_f Z^{-2/3} \ r_{TQ} A^{1/2} \ 2.7 \qquad (8c)$$

2.3.3 Scaling

The STREX data were available at the instrument height of 28 m, rather than 10 m. To make this data compatible with that from the other experiments, quantities were scaled down to values applicable at 10 m using the methods outlined below. First C_n^2 will be discussed, followed by temperature, humidity, and wind speed.

Eqn. (1) can be written in terms of P, T, structure function parameters and constants as:

$$C_n^2 = (k_1 P/T^2)^2 (C_T^2 + k_2 \ C_{TQ} + k_3 \ C_Q^2)$$

where $k_1 = 79 \times 10^{-6}$, $k_2 = .113$, $k_3 = 3.2 \times 10^{-3}$.

Substitution from Eqn (2) yields:

-24-

$$C_n{}^2 = \frac{P^2}{T^4} \left(Z^{-2/3} \, f(Z/L) \right) \left(T_*{}^2 + k_2 r_{TQ} \, T_* Q_* A^{1/2} + k_3 Q_*{}^2 A \right)$$

The scaling parameters T_* and Q_* do not vary with height in the su

The ratio of $C_n{}^2$ at 10 m to $C_n{}^2$ at an instrument height of Z_i m ca expressed:

$$\frac{C_{n_{10}}{}^2}{C_{n_{Z_i}}{}^2} = \frac{\dfrac{P_{10}{}^2}{T_{10}{}^4} \, (10^{-2/3}) \, f(10/L)}{\dfrac{P_{Z_i}{}^2}{T_{Z_i}{}^4} \, (Z_i{}^{-2/3}) \, f(Z_i/L)}$$

$(P_{10}/P_{Zi}) \approx 1$; $C_{n10}{}^2$ is thus:

$$C_{n10}{}^2 \approx C_{nZ_i}{}^2 \, \left(\frac{T_{Z_i}}{T_{10}}\right)^4 \, \left(\frac{10}{Z_i}\right)^{-2/3} \, \left(\frac{f(10/L)}{f(Z_i/L)}\right)$$

In the case of temperature and mixing ratio, using X to repr either quantity, Eqns (4b and 4c) lead to

$$\frac{X_{10}}{X_{Z_i}} = \frac{\left(\dfrac{X_*}{\alpha_T k}[\ell n(10/Z_{oT}) - \psi_2(10/L)] + X_o\right) \dfrac{\alpha_T k}{X_*}}{\left(\dfrac{X_*}{\alpha_T k}[\ell n(Z_i/Z_{oT}) - \psi_2(Z_i/L)] + X_o\right) \dfrac{\alpha_T k}{X_*}}$$

where the term $\alpha_T k/X_*$ has been added for simplification.
Solving for X_{10}, the scaling equation is:

$$X_{10} = X_{Z_i} \left(\frac{[\ell n(10/Z_{oT}) - \psi(10/L)] + X_o \dfrac{\alpha_T k}{X_*}}{[\ell n(Z_i/Z_{oT}) - \psi_2(Z_i/L)] + X_o \dfrac{\alpha_T k}{X_*}} \right)$$

To scale the wind Eqn (4a) is used in conjunction with the neutral stability drag coefficient, C_{DN}, which is defined as:

$$C_{DN}^{1/2} = k(\ln(Z'/Z_o))^{-1}$$

This can be solved for Z_o:

$$Z_o = Ze^{-k/C_{DN}^{1/2}} \tag{11}$$

From Eqn (4a) the ratio of the wind speed at 10 m to wind speed at Z_i m is:

$$\frac{U_{10}}{U_{Z_i}} = \frac{\dfrac{U_*}{k}\ [\ln(10/Z_o) - \psi_1(10/L)]}{\dfrac{U_*}{k}\ [\ln(Z_i/Z_o) - \psi_1(Z_i/L)]}$$

or,

$$\frac{U_{10}}{U_{Z_i}} = \frac{k\ C_{DN}^{-1/2} - \psi_1(10/L)}{\ln(Z_i/Z_o) - \psi_1(Z_i/L)}$$

substituting for Z_o from Eqn (11):

$$U_{10} = U_{Z_i} \frac{[K\ C_{DN_{10}}^{-1/2} - \psi_1(10/L)]}{[\ln(Z_i/10\ e^{-k\ C_{DN_{10}}^{-1/2}}) - \psi_1(Z_i/L)]} \tag{12}$$

2.4   RESULTS – C_n^2 VS REG PROFILE

In considering the results of the REG profile portion of the study it is well to keep in mind the number of days encountered with each profile type. Table 5 lists the number of days of each REG profile, along with the number of hourly averaged observations.

TABLE 5

REG Breakdown of Observations

REG Profile	Number of Days	Number of Observations
B	35	467
C	4	69
D	55	648
E	24	400
F	10	142
J	9	106
K	40	534

It is sometimes quite difficult to distinguish between E and F days using synoptic maps to classify a location according to the REG. In view of this the two profile types were grouped together. The relatively low number of observations in the C and J categories should be remembered when considering results which are determined according to hour of the day. The units of C_n^2 values presented in this report will always be $m^{-2/3}$.

Figure 3 is a cumulative frequency plot. We believe this can give much insight into the distribution of C_n^2 for various REG categories. Table 6 lists C_n^2 values at the 75%, 50% and 25% levels as shown in the graph.

TABLE 6

Cumulative Frequency of C_n^2

REG Profile	75%	50%	25%
B	$7.9 \times 10^{-16} \, m^{-2/3}$	$1.0 \times 10^{-15} \, m^{-2/3}$	$4.0 \times 10^{-15} \, m^{-2/3}$
C	6.3×10^{-16}	1.6×10^{-15}	3.5×10^{-15}
D	1.5×10^{-16}	1.0×10^{-15}	3.7×10^{-15}
E&F	6.3×10^{-16}	1.6×10^{-15}	3.2×10^{-15}
J	1.3×10^{-16}	5.0×10^{-16}	1.6×10^{-15}
K	2.5×10^{-16}	1.6×10^{-15}	6.3×10^{-15}
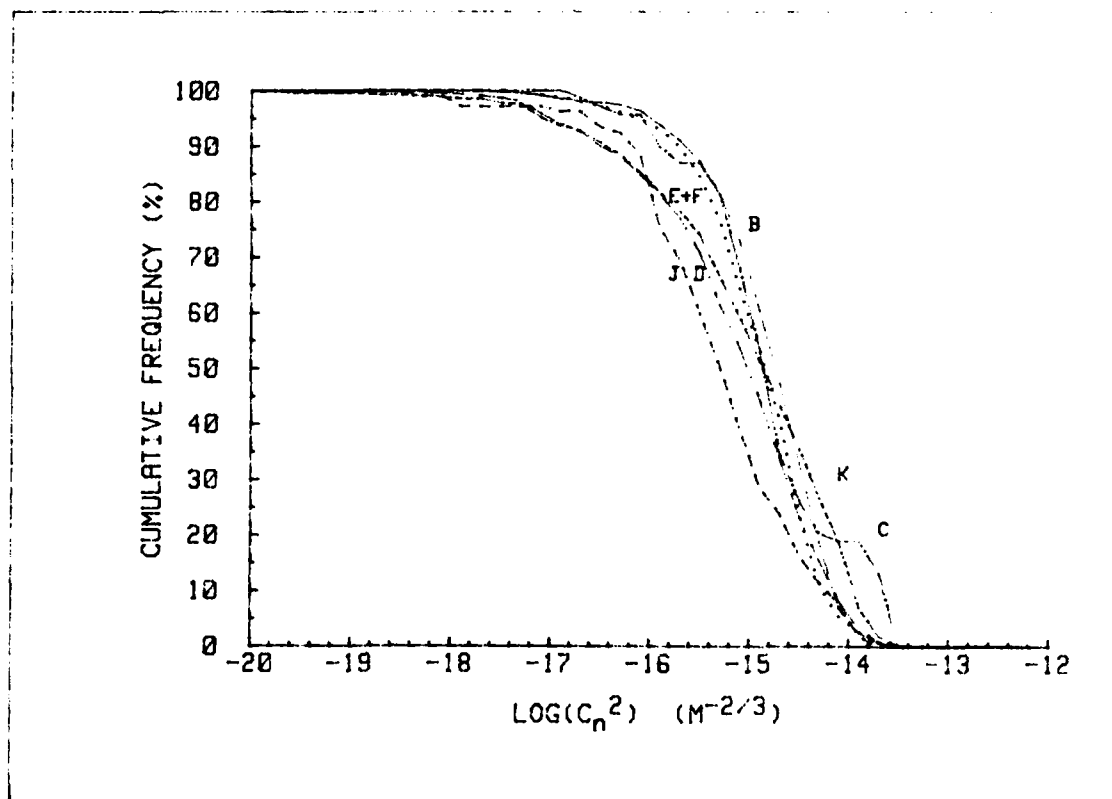
Figure 3. Cumulative frequencies of log ($C_n{}^2$) according to REG
regimes.

Table 6 and Fig. 3 illustrate that even for category J 25% of the time light turbulence can be expected; values for K profiles are much larger at this level.

Another way to interpret Fig. 3 is to consider what percentage of C_n^2 values are larger than a certain threshold value. Table 7 shows that for REG profiles C and K it will not be uncommon to encounter values greater than 1×10^{-14}. For all categories, values greater than 1×10^{-15} will frequently occur.

TABLE 7

Percentage of C_n^2 Values Greater Than Threshold

Threshold: $(m^{-2/3})$	1×10^{-15}	1×10^{-14}
REG Profile	%	%
B	68	5
C	61	19
D	50	5
E&F	60	5
J	34	5
K	56	13

Figure 4 shows the frequency distribution of each REG profile. In nearly all categories a sharp cut-off exists at the high end; the low end of the curve often trails off in a long tail. Categories B and E&F present sharply peaked curves, while the distributions for D, J and K are more spread out. Due to the relatively small sample size for type C it is difficult to determine to which group it belongs. Profiles C, D, and K have the largest values of C_n^2 associated with them. K occurs around the center of a low pressure system; D profiles are found after the passage of a cold front, and C is associated with a polar air mass (see Figure 1).

Figure 4. Frequency distribution of log (C_n^2) according to REG categories.

REG CATEGORY D

c

REG CATEGORIES E & F

d

e

f
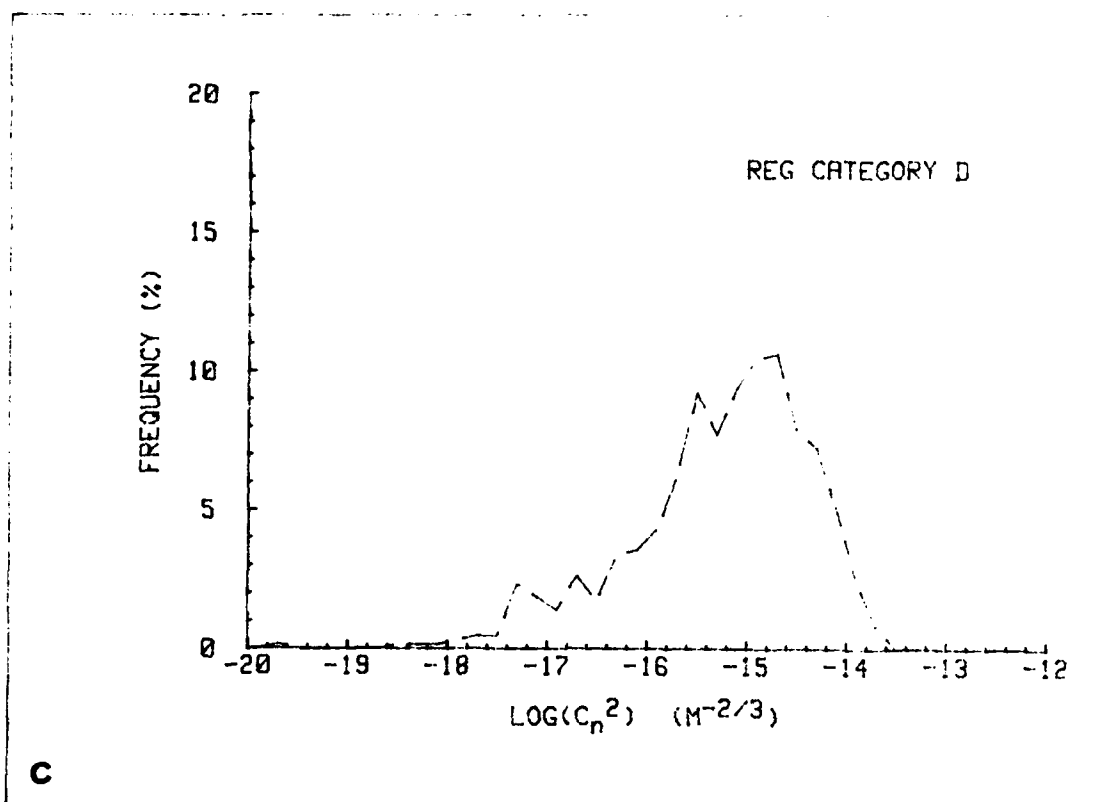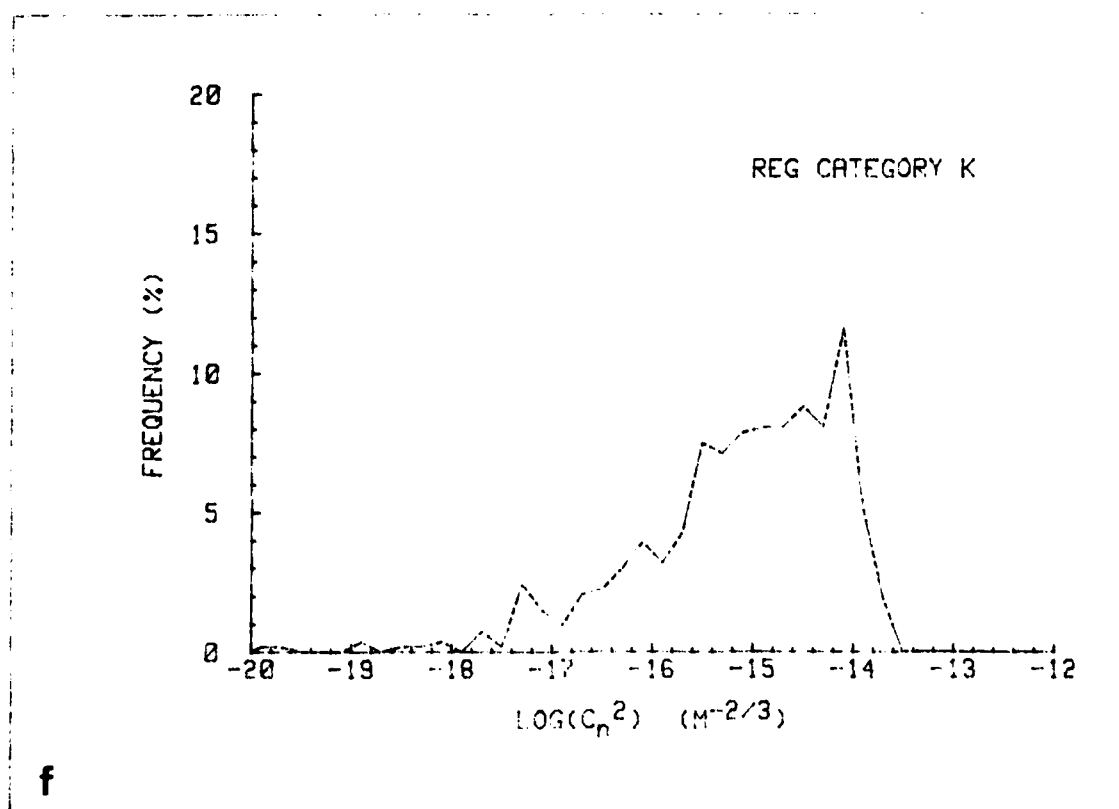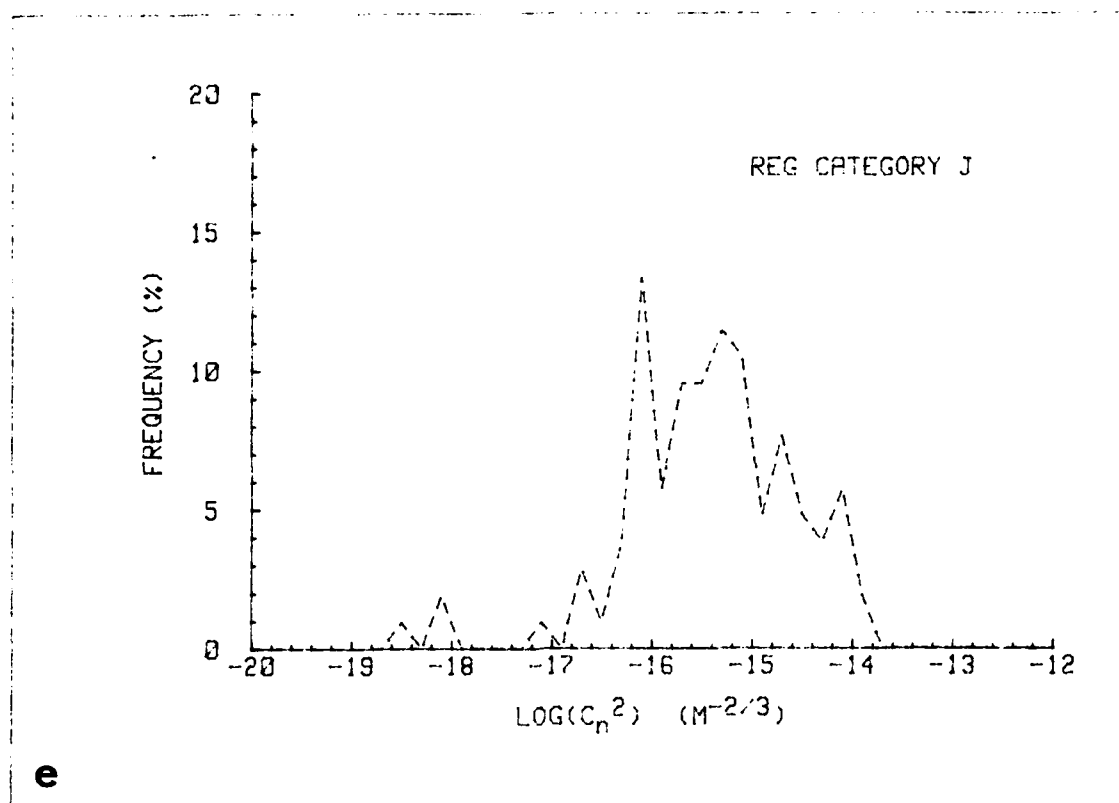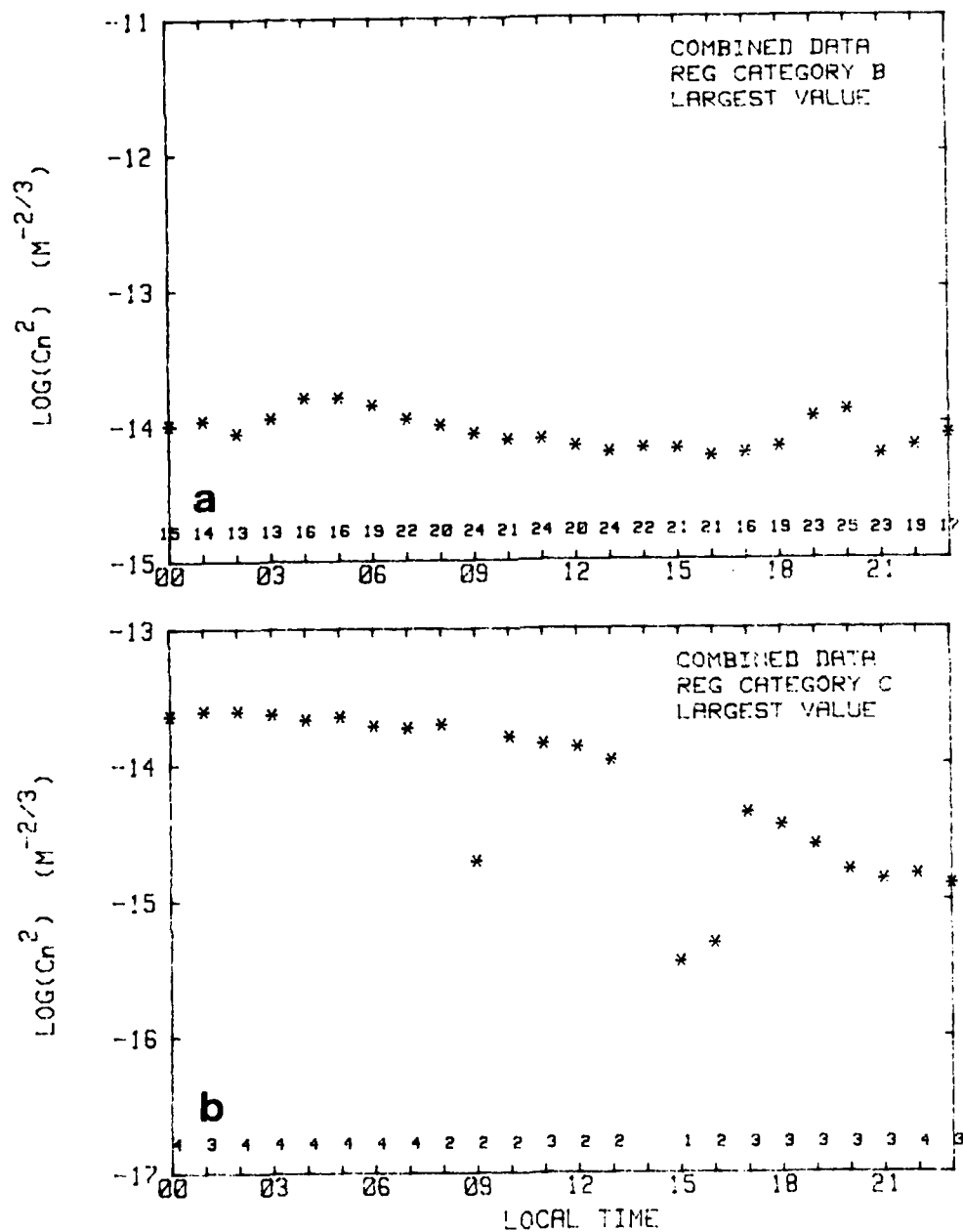
Figure 5. Logarithm of largest values of C_n^2 encountered each hour
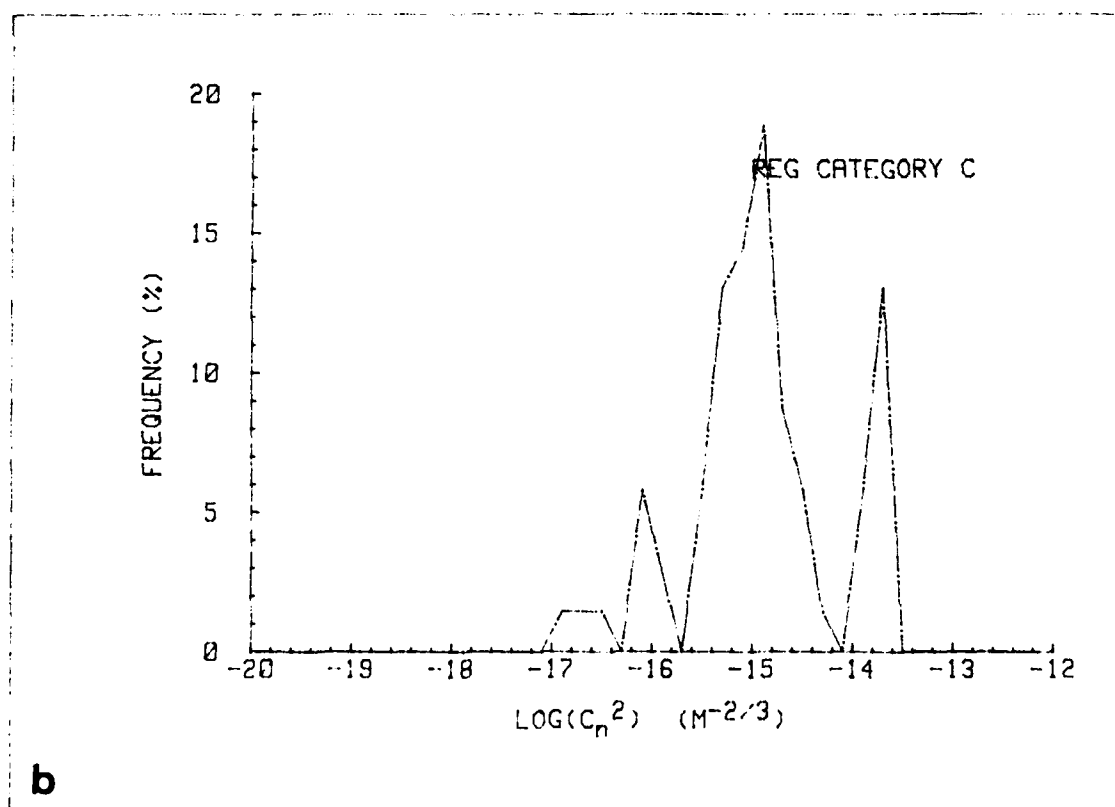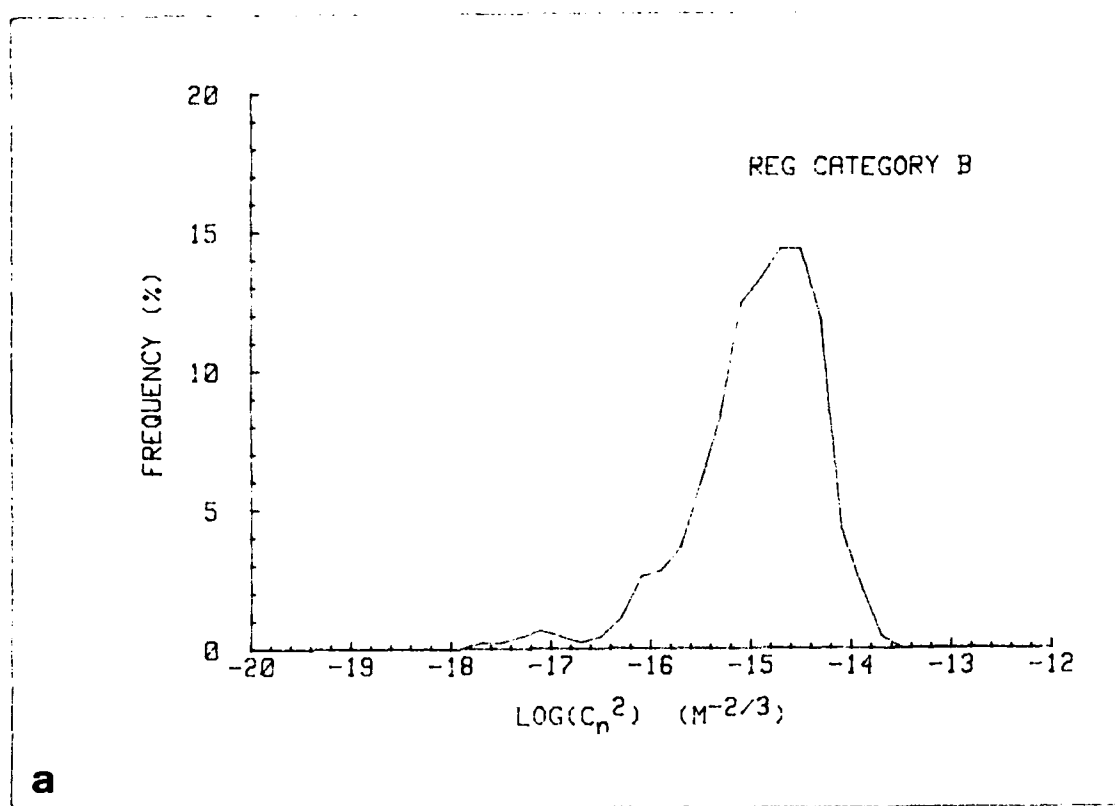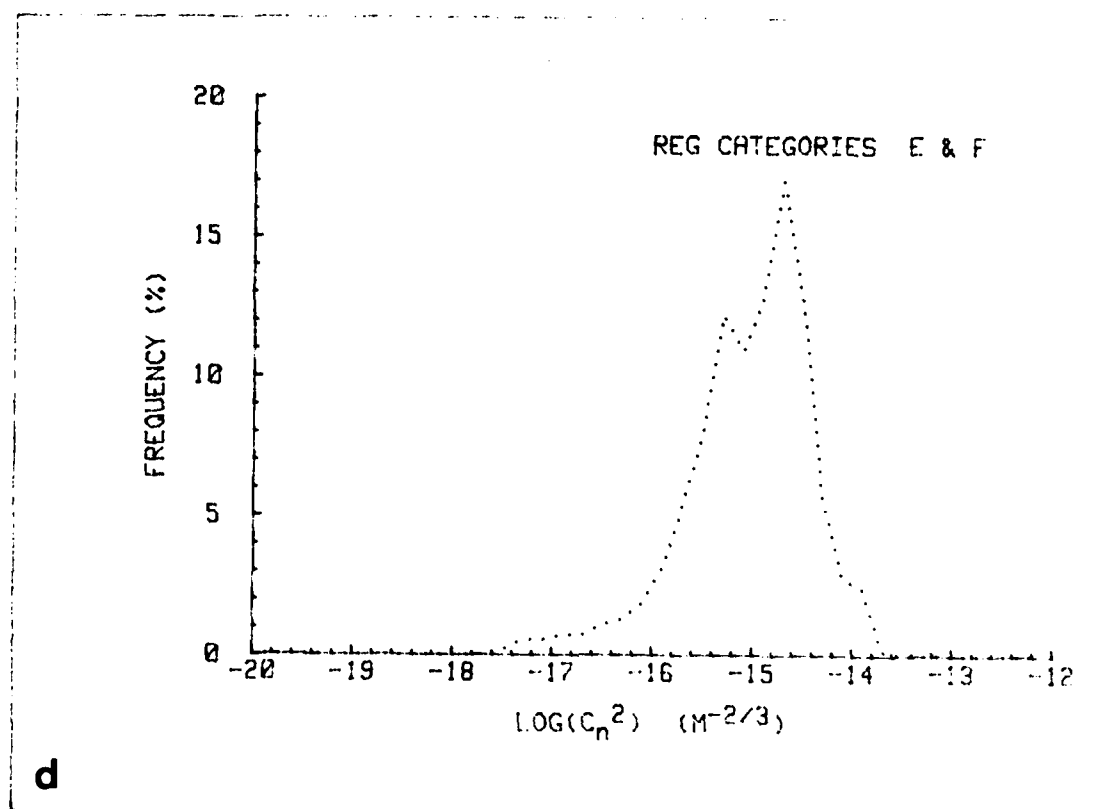during all days entire data set with specified REG profile.
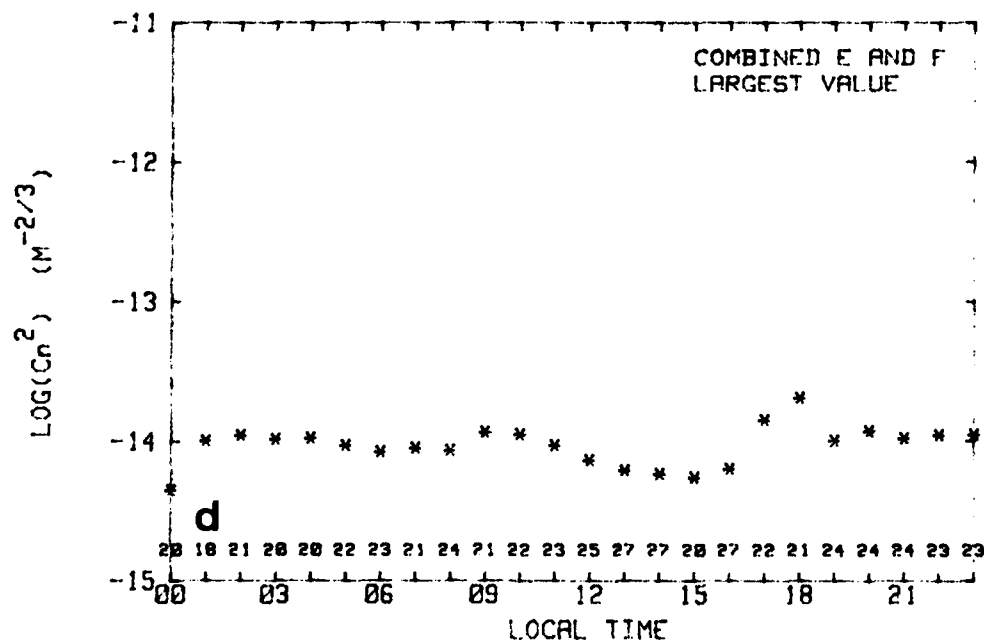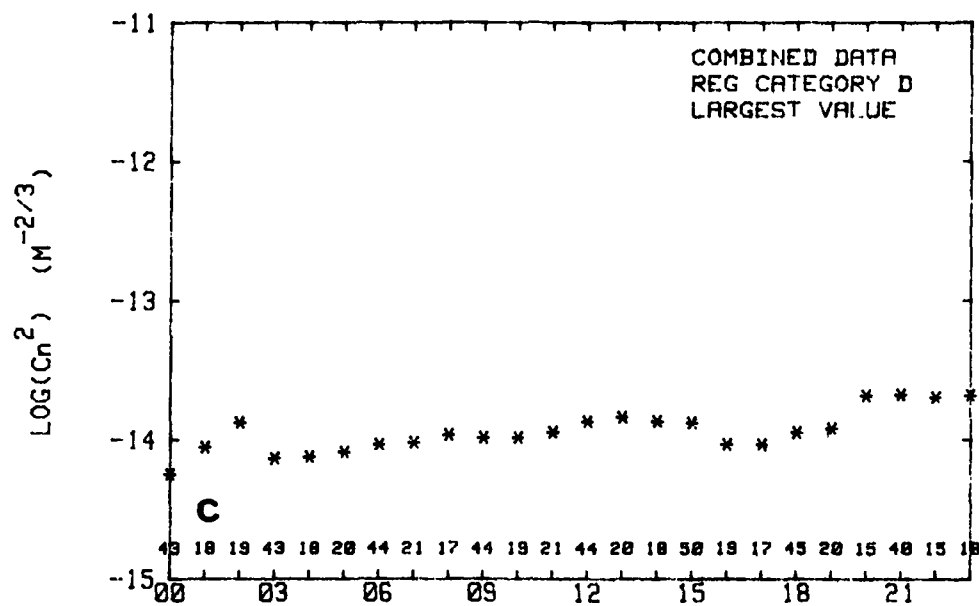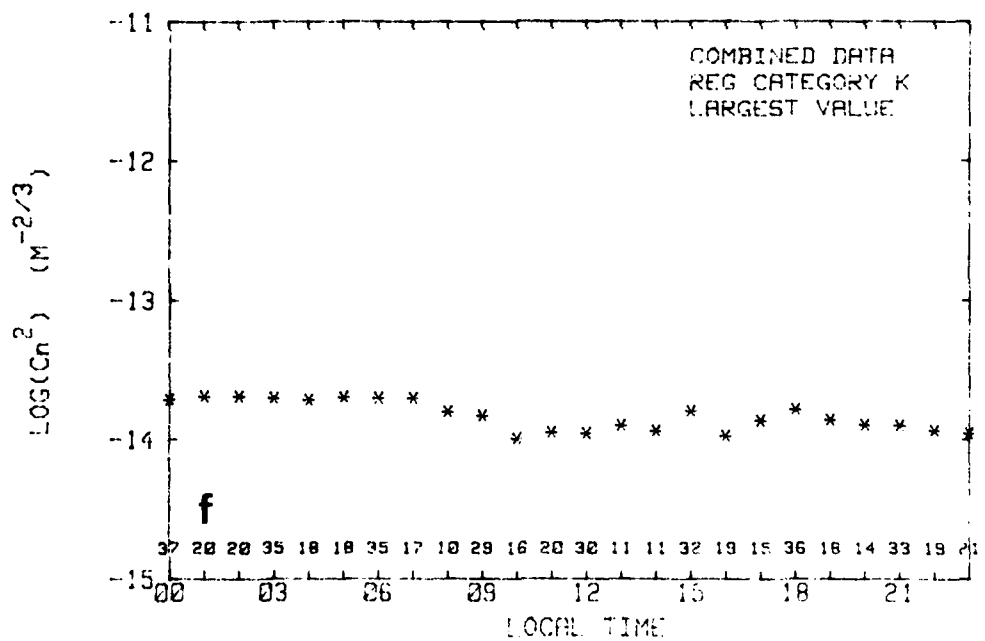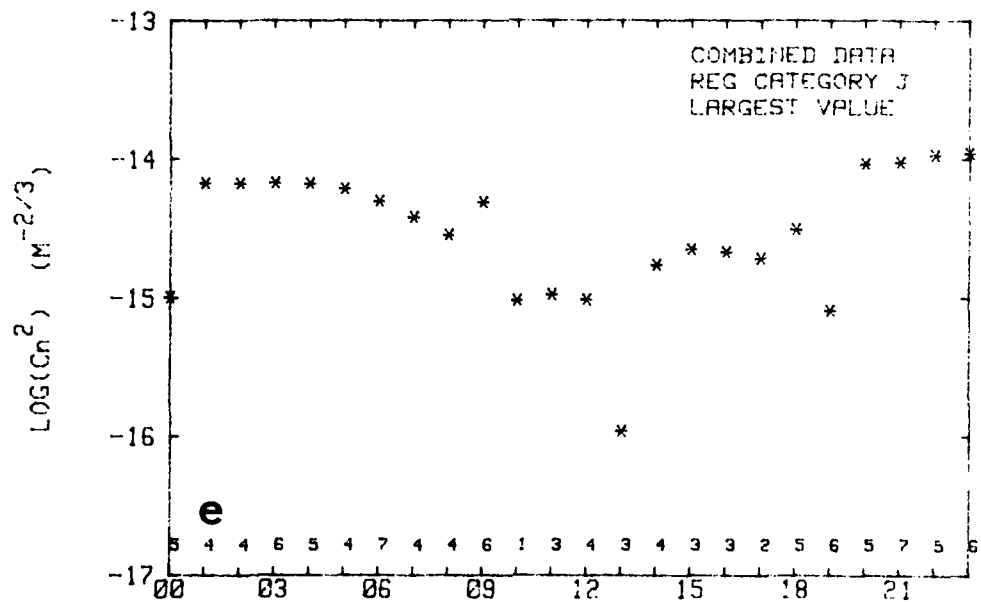
Considering $C_n{}^2$ on a diurnal basis, Fig. 5 presents the largest $C_n{}^2$ value found at each hour of the day, according to the REG category. The small numbers along the bottom of the graphs are the number of hourly averaged observations available at each hour. It is obvious from Fig. 5 as it was from Fig. 4 that the largest values are found with profiles C, D, and K. Furthermore, there is no apparent diurnal variation in the maximum value. J has lower maxima than any other REG profile type; however, the small sample size for J may have contributed to this result.

Turning next to the mean values of $C_n{}^2$, Fig. 6 again shows no diurnal variation. The error bars in Fig. 6 are the standard deviation of the mean. There is not enough data at each hour for types C and J to give any insight into their mean values. REG regime K appears to have slightly higher mean values than the other regimes. There is very little difference between the mean values of profiles B, D and E&F. The oscillatory nature of the K graph is thought to be due to the fact that K days were encountered mainly in two experiments, JASIN and STREX. Most of the JASIN data were available at 3-hour intervals (the hours at which the lowest means occur). It is not known for certain whether the variation in mean values is due to differing atmospheric conditions between the two experiments (JASIN occurred during summer in the North Atlantic, and STREX during winter in the Gulf of Alaska) or different data handling techniques. The fact remains in either case that profile K has slightly higher mean values than the other regimes.
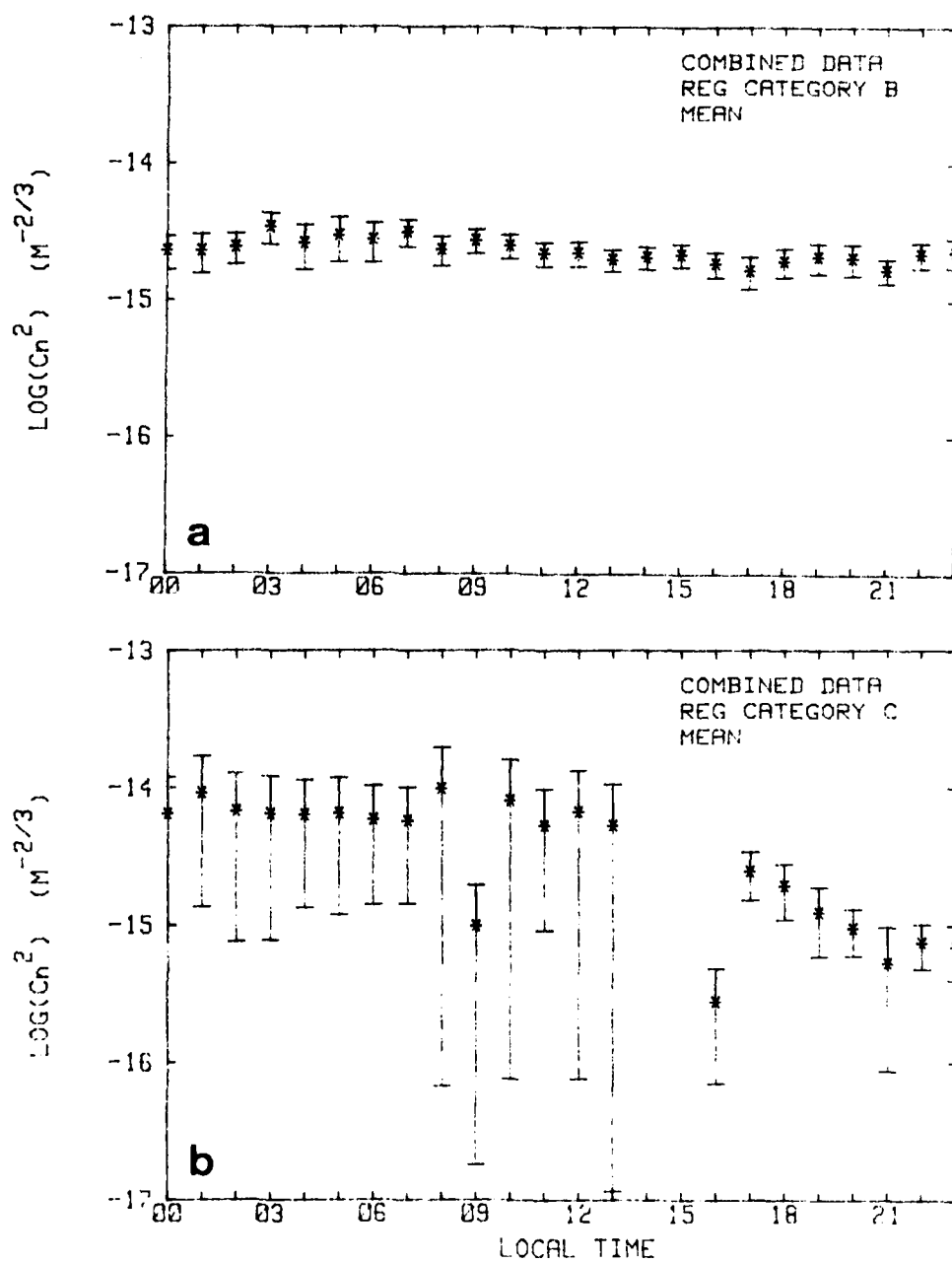
Figure 6.   As in 5, except logarithm of mean values.   Bars indicate
standard deviation.

COMBINED DATA
REG CATEGORY D
MEAN

c

COMBINED E AND F
MEAN

d
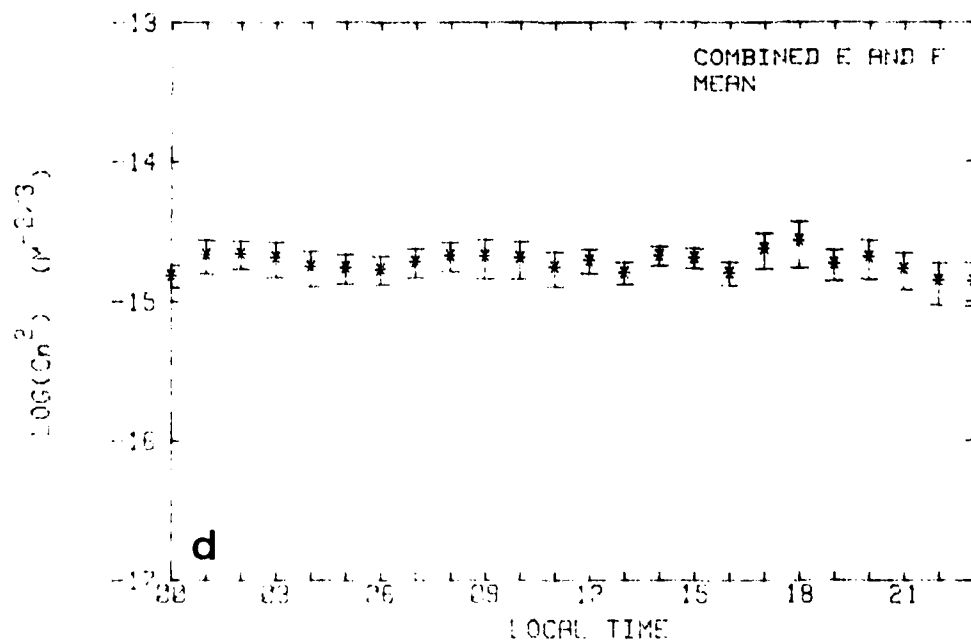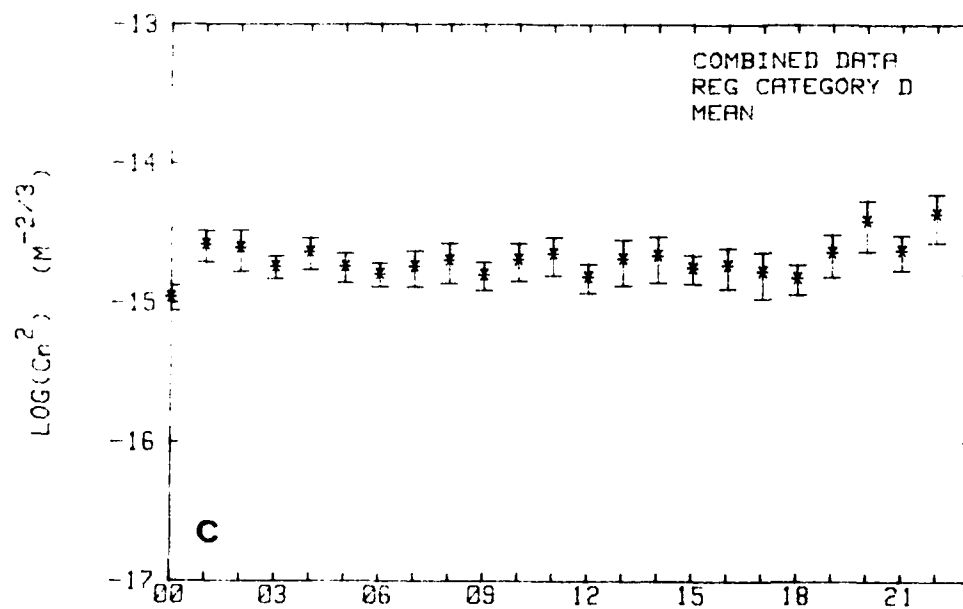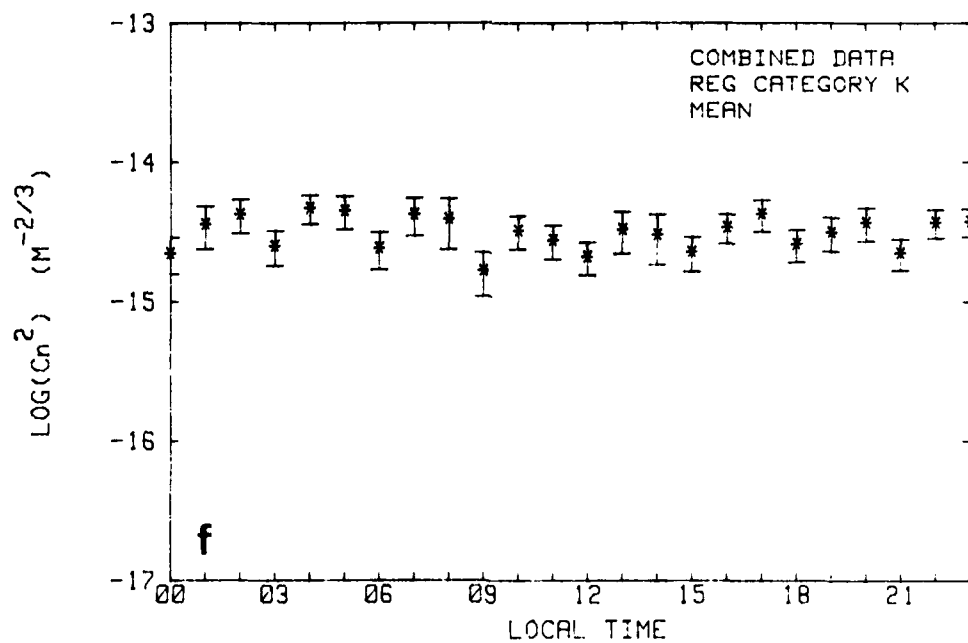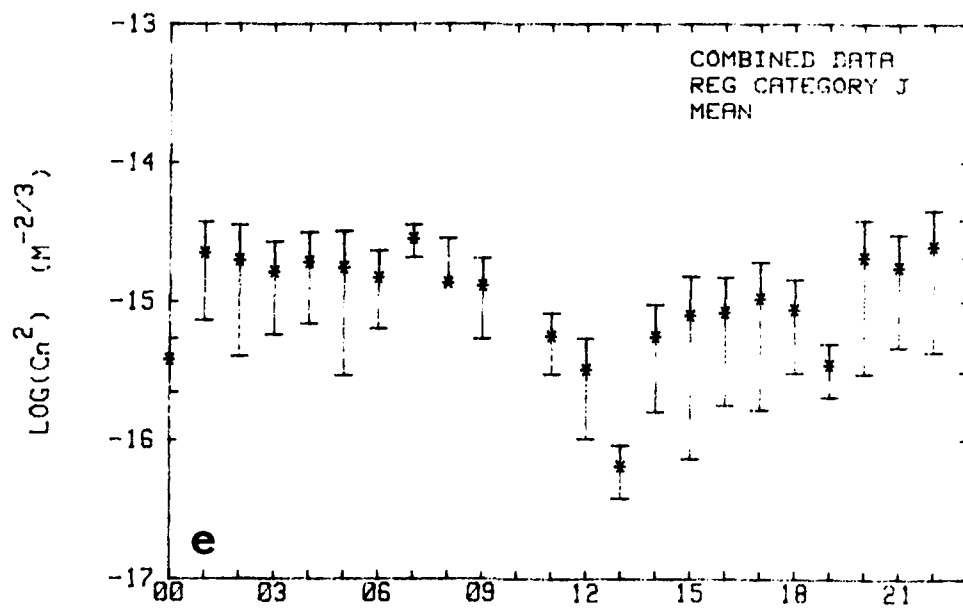
3. HORIZONTAL HOMOGENEITY OF C_n^2

3.1 METEOROLOGICAL DATA

3.1.1 Experimental Location

Surface layer C_n^2 was studied with respect to horizontal homogeneity using data from the 1978 JASIN experiment. Concurrent data were available every three hours from three ships during two periods of time. The latitude and longitude of the corners and center of the triangle were as follows:

NW	60.25N	14.5W
NE	60.25N	10.5W
S	59.00N	12.5W
Center	59.77N	12.5W

The length of each leg is approximately 200 km. A ship was stationed at each corner.

The first period (Case I) was 45 hours long, from 7 August 0000 GMT to 8 August 2100 GMT. Case II extended for two weeks, from 22 August 0000 GMT to 4 September 1800 GMT. Data were collected from the same area in both cases. Figure 7 shows the experimental area in the North Atlantic. The ship at the northwest corner of the JASIN triangle throughout the experiment was the GARDENER ENDURER; the METEOR was at the south corner. During Case I the JOHN MURRAY was stationed at the northeast corner while HECLA was the northeast ship during Case II.

3.1.2 Data Acquisition and C_n^2 Calculations

Meteorological measurements made aboard all four ships involved in this portion of the study were described in Section 2.2.2 and included measures of air and sea-surface temperatures, humidity, wind speed and temperature. Section 2.3.1 outlined the application of the bulk aerodynamic method in estimating C_n^2 from the JASIN data.
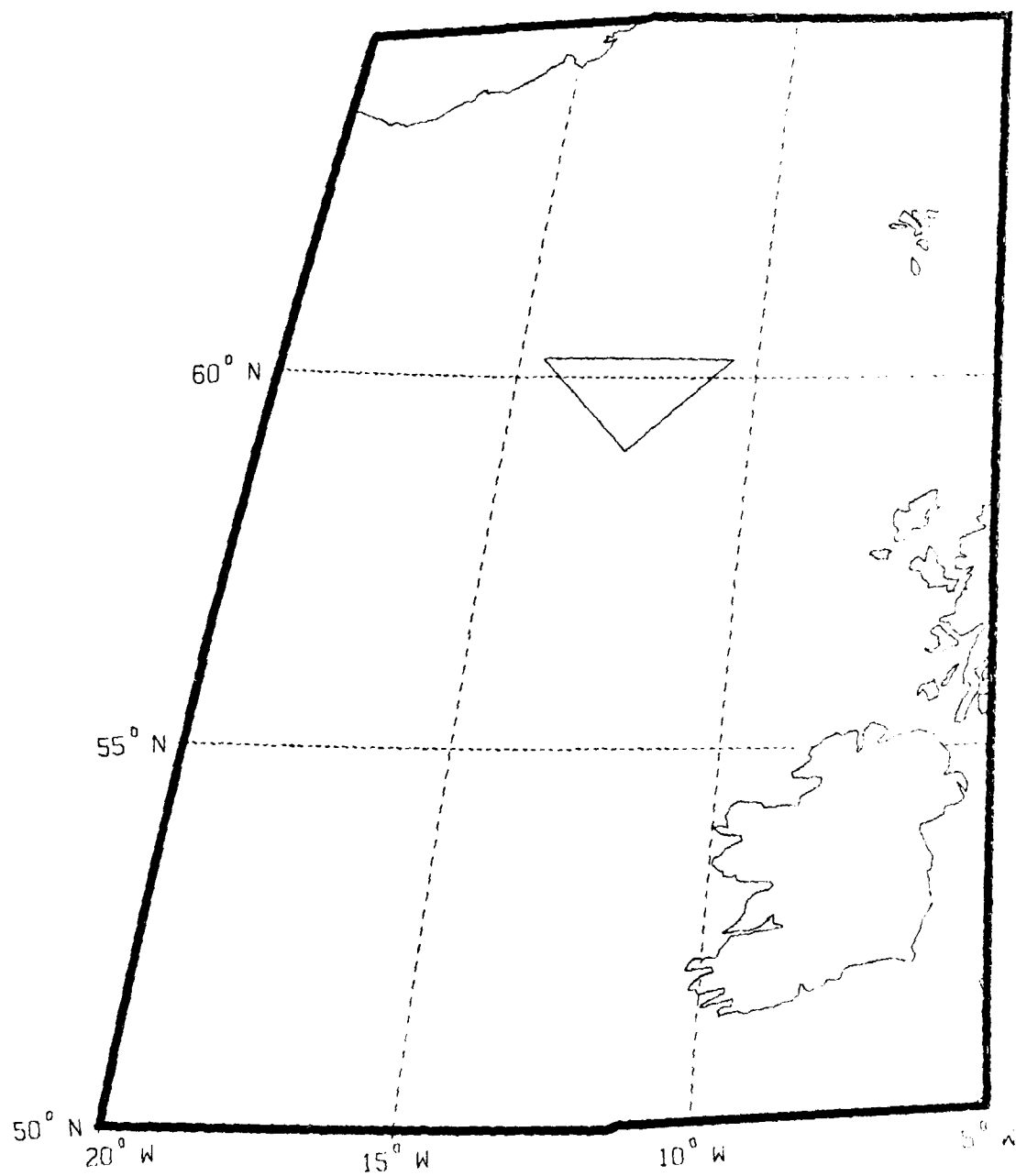
Figure 7. Experimental area during JASIN.

3.2   HORIZONTAL HOMOGENEITY DETERMINATION

The bulk method has been verified for calculating optical turbulence over water by Davidson et al. (1981). It was determined that values of C_n^2 can be estimated to within a factor of 2 using the bulk method in equilibrium situations. This range includes inaccuracies due to instrument errors. It is assumed here that the atmosphere was generally in equilibrium in the region of the JASIN triangle during both Case I and Case II.

Given the factor of 2 accuracy, a bulk estimate of C_n^2 will fall in the range

$$\frac{1}{2} C_{n_{True}}^2 \leq C_{n_{Bulk}}^2 \leq 2C_{n_{True}}^2$$

or, in log space,

$$\log C_{n_{True}}^2 - \log 2 \leq C_{n_{Bulk}}^2 \leq \log C_{n_{True}}^2 + \log 2$$

With an error in $\log C_{n_{Bulk}}^2$ of log 2, horizontal homogeneity of C_n^2 between two points A and B was assumed to exist if:

$$\left| \log C_{n_A}^2 - \log C_{n_B}^2 \right| \leq \sqrt{(\log 2)^2 + (\log 2)^2} \tag{13}$$

The criterion in Eqn (13) was used to determine periods of horizontal homogeneity in C_n^2 along each leg, or sector, of the JASIN triangle. The sectors were labeled as shown below:
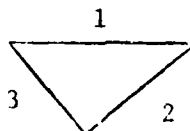
Sector homogeneity was determined for each measurement period by applying Eqn (13) to the bulk C_n^2 values calculated for the two ships at either end of the sector.

If sector homogeneity existed along all three sectors during a measurement period, then areal homogeneity was said to exist for that measurement time.

3.3   SYNOPTIC SITUATION AND REG REGIME

During Case I the JASIN triangle was under the influence of a high pressure ridge which drifted to the east as a trough approached. Surface winds were northerly and light. Both 7 August and 8 August were classified as REG type D days in the area. Figure 8a shows surface weather maps for Case I with the experimental area indicated by the triangle.

The Case II situation was more variable. On 22 August a cold front approached which passed over the area on 23 August. This was followed by cold, dry air which persisted through 24 August. On 25 August the humidity increased as a warm front approached and passed through the triangle. The region was dominated by a high pressure system from 26 through 28 August when an occluded front slowly neared. This passed by on 29 August bringing colder, drier air. The area was in a warm sector on 30 August, then a cold front passed through early on 31 August. Late on 1 September a warm front approached which went through the area the next day. Another warm front approached on 3 September and passed through on 4 September.

Most of the days during this Case were classified as REG D profile days. The exceptions were 2 and 4 September which were J days, and 3 September which was a K day. Figure 8b shows surface weather maps for Case II.

3.4   RESULTS – HORIZONTAL HOMOGENEITY OF C_n^2

3.4.1 Episodes of Surface Layer Homogeneity

As expected, horizontal homogeneity of surface layer C_n^2 existed more often along individual legs of the JASIN triangle than over the entire area. The percentage of measurement periods (hourly averages, available every three hours), during which areal homogeneity existed was larger in Case I than Case II; the latter period was much longer and included several different weather patterns.

DAILY WEATHER MAPS

(12 GMT) 2 – 16 AUGUST 1978
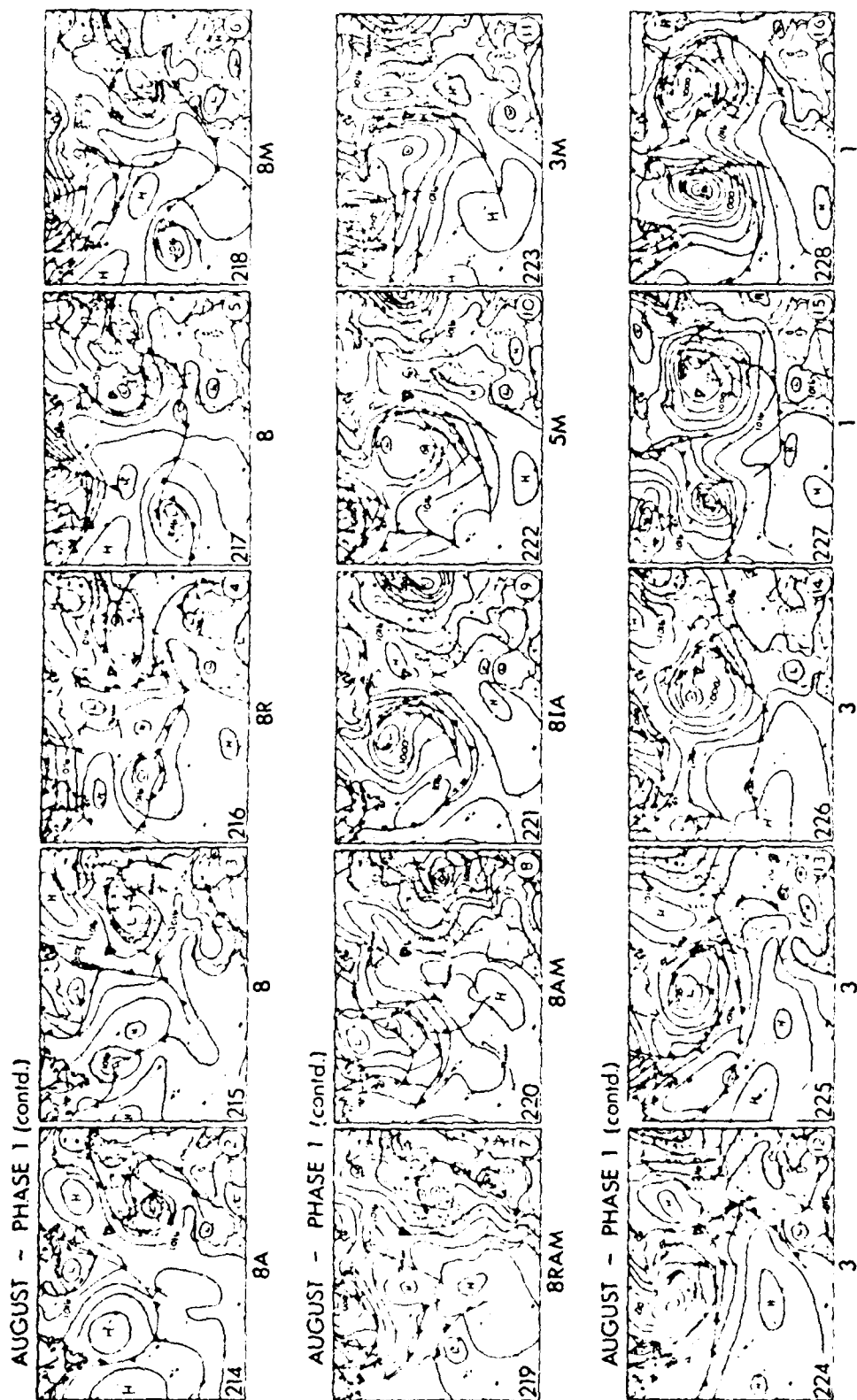
AUGUST – PHASE 1 (contd.)

AUGUST – PHASE 1 (contd.)

AUGUST – PHASE 1 (contd.)

n = no. of ships on station .   R = intensive radiosondes .   A = aircraft operating .   I = full intercomparison .

M = oceanographic multiship experiment

a   Figure 8.   Surface synoptic maps during a) Case I and b) Case II of JASIN.

-45-

DAILY WEATHER MAPS

(12 GMT)   17 – 31 AUGUST 1978

AUGUST – PHASE 2

229	230	231	232	233
2	1	7	8I	9A
17	18	19	20	21

AUGUST – PHASE 2 (contd.)

234	235	236	237	238
10RA	10A	12RA	13RA	13
22	23	24	25	26

AUGUST – PHASE 2 (contd.)

240	241	242	243
14RM	14AM	12AM	12RAM
28	29		31
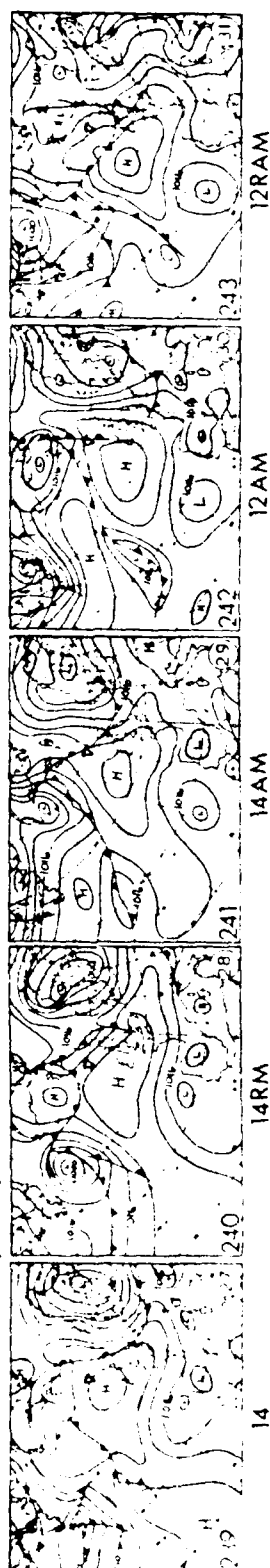
n = no. of ships on station ,   R = intensive radiosondes ,   A = aircraft operating ,   1 = full intercomparison ,

M = oceanographic multiship experiment

-46-

DAILY WEATHER MAPS

(12 GMT) 1 - 15 SEPTEMBER 1978

SEPTEMBER - PHASE 2 (contd.)
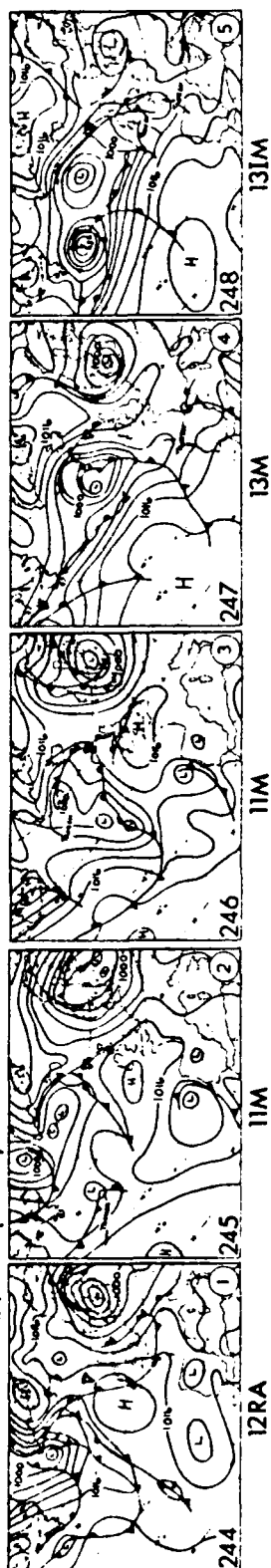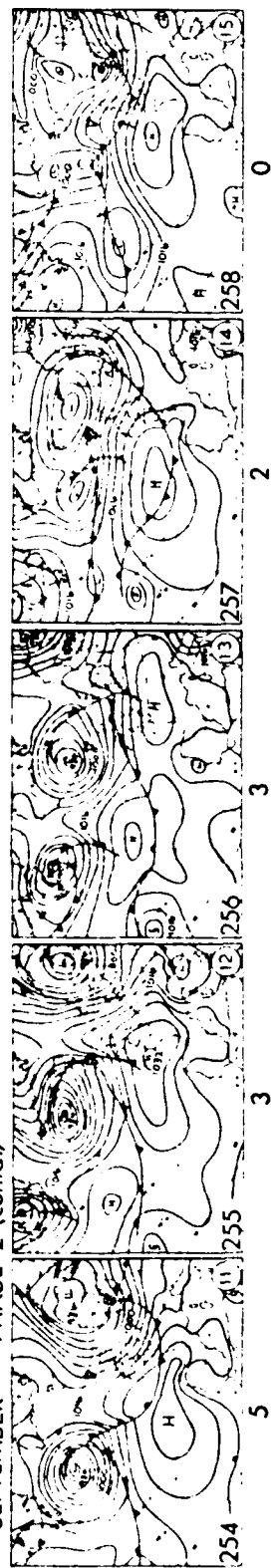
SEPTEMBER - PHASE 2 (contd.)

SEPTEMBER - PHASE 2 (contd.)

n = no. of ships on station , R = intensive radiosondes , A = aircraft operating , I = full intercomparison .

M = oceanographic multiship experiment

b (cont'd)

Figure 9 indicates for both cases the percentage of measurement periods during which horizontal homogeneity existed along each sector and over the entire area.

Case I

37.5

37.5

43.8   100.0

Case I:

40.2

11.8

38.2   26.5
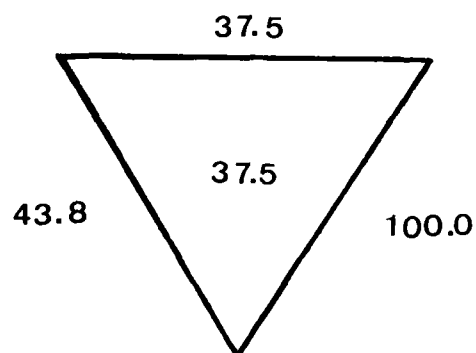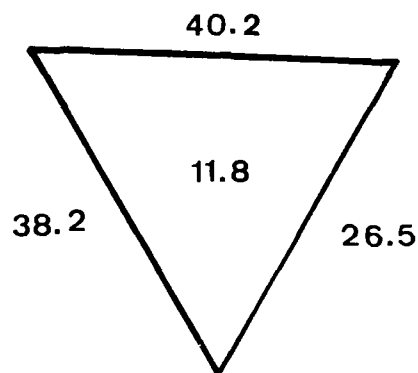
Figure 9.   Percentage of measurement periods in which sector and horizontal homogeneity of C_n^2 existed during Case I and Case II of JASIN.

This figure illustrates the fact that horizontal homogeneity in surface layer C_n^2 can exist over 200 km for periods as long as 45 hours (Sector 2 Case I). Table 8 lists all the episodes of homogeneity for Case I.

Table 8

Periods of Horizontal Homogeneity of C_n^2 during Case I

Sector 1	Sector 2	Sector 3	Areal
7 Aug 0000-0000[*]	7 Aug 0000-	7 Aug 0000-0000[*]	7 Aug 0000-0000[*]
7 Aug 0600-0900	8 Aug 2100	7 Aug 0600-2100	7 Aug 0600-0900
7 Aug 1500-2100			7 Aug 1500-2100

[*] only one measurement period indicated homogeneity

Case II results are shown in Fig. 10. The leftmost set of bars are for cases in which homogeneity existed during only 1 measurement period, the second set arises from 2 consecutive homogeneous measurement periods, and so on. It can be seen that it is possible to have homogeneity in C_n^2 over the whole area for periods lasting between 9 and 12 hours, although such a case is rare.

3.4.2 Factors Influencing Homogeneity

Since nearly all of the days involved in both Cases studied here were REG D days it was not possible to determine the relationship, if any, between the REG classification and horizontal homogeneity in C_n^2. In addition, there was no clear pattern evident when comparing episodes of homogeneity with the synoptic situation. This is not surprising; since C_n^2 values are so sensitive to changes in small scale quantities such as the air-sea temperature difference one would expect local factors to play an important part in homogeneity.
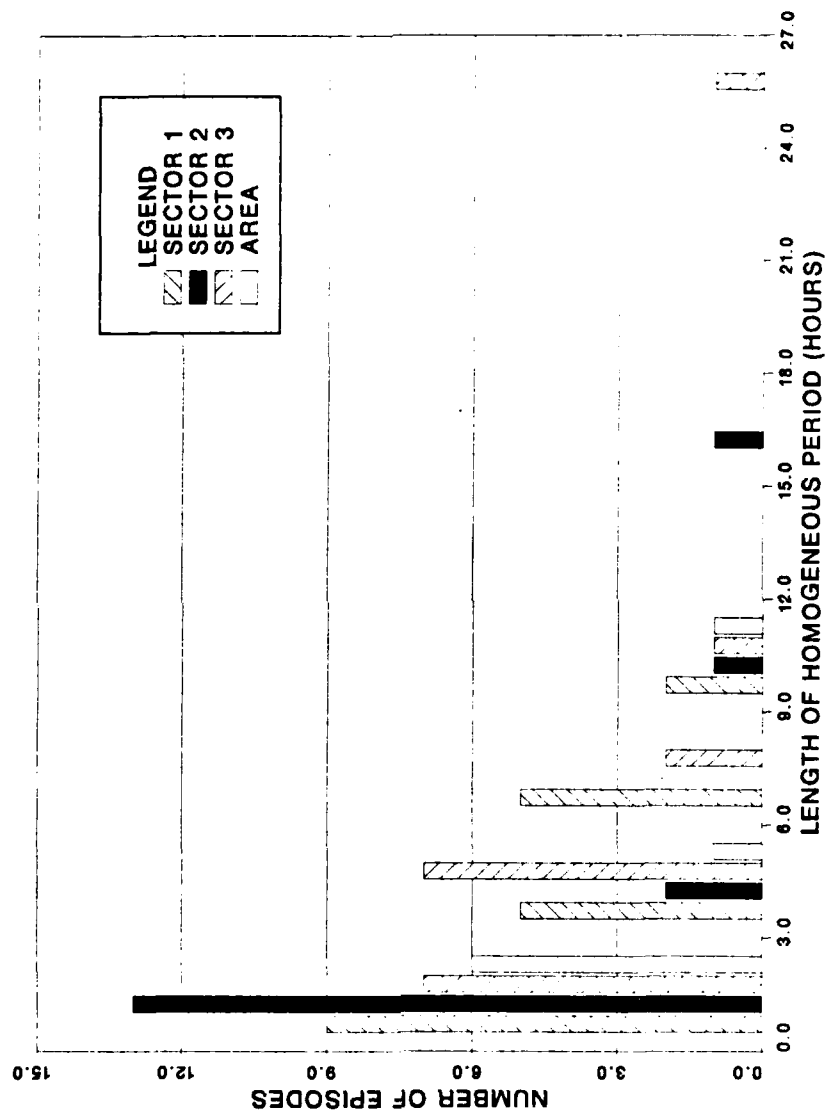
Figure 10. Number and duration horizontally homogeneous C_n^2 episodes during Case II of BASIN.

In view of the above, several quantities were examined using the hourly averaged data from all three ships in the JASIN triangle to determine which factors were most important in affecting the homogeneity of C_n^2 in the region. The quantities studied included gradients along each sector as well as mean values at each ship.

For each ship, the mean wind speed and mean air-sea temperature difference were calculated during periods of sector and areal homogeneity and non-homogeneity. Gradients in wind, air temperature, sea temperature and air-sea temperature difference along each sector were also calculated for the same periods. The results of the analysis for both Cases are shown in Table 9.

The most important factor affecting homogeneity in C_n^2 appears to be the gradient in air-sea temperature difference. The other factors do not seem to have a great influence on C_n^2 homogeneity. Generally, the gradient in air-sea temperature difference was less than .8C per 200 km during times of homogeneity and greater than 1C per 200 km when homogeneity did not exist.

Table 9

Mean Quantities at Each Ship

Areal Study

Homogeneous ¦ Non-Homogeneous	ENDURER		MURRAY		METEOR	
CASE 1						
Wind (m/s)	3.97	2.00	7.50	6.30	5.59	5.45
Air-Sea Temp(C)	-2.32	-1.61	-1.90	-2.36	-2.08	-2.41

	ENDURER		HECLA		METEOR	
CASE 2						
Wind (m/s)	7.71	6.31	6.89	6.49	7.40	6.19
Air-Sea Temp(C)	-0.78	-0.78	0.01	0.03	-0.68	-0.36

Sector Study

SECTOR 1

Homogeneous ¦ Non-Homogeneous	ENDURER		MURRAY	
CASE 1				
Wind (m/s)	3.97	2.00	7.50	6.30
Air-Sea Temp(C)	-2.32	-1.61	-1.90	-2.36

	ENDURER		HECLA	
CASE 2				
Wind (m/s)	6.07	6.65	6.04	6.77
Air-Sea Temp(C)	-0.86	-0.72	-0.24	-0.17

SECTOR 2

Homogeneous ¦ Non-Homogeneous	MURRAY		METEOR	
CASE 1				
Wind (m/s)	6.75	--	5.50	--
Air-Sea Temp(C)	-2.19	--	-2.29	--

	HECLA		METEOR	
CASE 2				
Wind (m/s)	6.74	6.45	7.38	6.13
Air-Sea Temp(C)	0.01	0.28	-0.56	-0.34

Table 9 Cont'd

Mean Quantities at Each Ship (Cont'd)

Sector Study (Cont'd)

SECTOR 3

Homogeneous¦Non-Homogeneous		ENDURER		METEOR	
CASE 1	Wind (m/s)	3.68	2.00	5.76	5.30
	Air-Sea Temp(C)	-2.04	-1.47	-2.03	-2.49

		ENDURER		METEOR	
CASE 2	Wind (m/s)	7.03	6.09	7.34	5.76
	Air-Sea Temp(C)	-0.74	-0.79	-0.54	-0.29

Gradients Along Sectors (x 200 m)

Areal Study

Homogeneous¦Non-Homogeneous		Sector 1		Sector 2		Sector	
CASE 1	Air Temp(C)	0.75	1.96	1.50	1.63	0.77	0
	Sea Temp(C)	1.15	1.20	1.68	1.68	0.63	0
	Wind (m/s)	3.53	4.30	1.91	1.06	1.62	3
	Air-Sea Temp(C)	0.44	1.07	0.30	0.37	0.50	1
CASE 2	Air Temp(C)	0.51	0.64	0.56	0.79	0.38	0
	Sea Temp(C)	0.82	0.92	1.05	0.97	0.25	0
	Wind (m/s)	2.19	1.60	1.42	1.65	1.55	1
	Air-Sea Temp(C)	0.88	1.10	0.79	1.00	0.23	0

Sector Study

Homogeneous¦Non-Homogeneous		Sector 1		Sector 2		Sector	
CASE 1	Air Temp(C)	0.75	1.96	1.58	--	0.91	0.
	Sea Temp(C)	1.15	1.20	1.68	--	0.63	0.
	Wind (m/s)	3.53	4.30	1.38	--	2.07	3.
	Air-Sea Temp(C)	0.44	1.07	0.35	--	0.60	1
CASE 2	Air Temp(C)	0.62	0.63	0.62	0.71	0.42	0.
	Sea Temp(C)	0.70	1.02	0.96	1.02	0.23	0.
	Wind (m/s)	1.57	1.84	1.70	1.54	1.61	1.
	Air-Sea Temp(C)	0.80	1.23	0.76	1.13	0.34	0.

4. CONCLUSIONS AND RECOMMENDATIONS

Considering first the results of the REG profile portion of this study, it has been shown that light turbulence (values of C_n^2 greater than 10^{-15} $m^{-2/3}$) occur over the ocean a significant percentage of the time. This is true of all REG regimes studied. Profile types C and K were seen to have values of C_n^2 greater than 10^{-14} $m^{-2/3}$ quite often, a level of turbulence which can seriously affect the performance of EO systems.

It was seen that certain REG regimes (B and E&F) have more sharply peaked distributions than other regimes. The range of C_n^2 values between the 25th and 75th percentile for these regimes is smaller; it may be easier to predict expected values for these categories than other REG profiles.

No diurnal trend was found in any REG category in either the mean values of C_n^2 over the ocean or the largest value encountered on an hourly basis. The largest values were found to occur with REG types C, D and K. Profile K also had the greatest mean values of C_n^2 when the data were examined hour by hour. There was no apparent difference in the hourly mean values for types B, D and E&F. There was not enough data for categories C and J to make any conclusions about their hourly mean values.

Based on the above results it is concluded that the REG does not contain enough detail to consistently separate periods of differing levels of optical turbulence as reflected by values of C_n^2 for every REG category. However, the REG can be useful in predicting ranges and expected values of C_n^2 for certain groups of REG regimes as discussed above (e.g. profiles C and K were associated with C_n^2 values greater than 10^{-14} $m^{-2/3}$ more often than were other profiles). More local factors must be included in a detailed C_n^2 prediction scheme.

In examining the horizontal homogeneity of surface layer C_n^2 it was found that homogeneity can, rarely, persist in an area the size of the JASIN triangle for more than 9 hours; it can occasionally last for 1 to 2 days along a 200 km sector. Horizontal homogeneity of C_n^2 seems to be affected mainly by gradients in air-sea temperature difference along a sector.

It might be valuable to further investigate the causes of horizontal homogeneity of surface layer C_n^2, considering the number of homogeneous episodes which were found to persist for up to half a day.

References

Businger, J. A., 1973: "Turbulent Transfer in the Atmospheric Surface Layer", Workshop on Micrometeorology, Amer. Met. Soc. Publication, Science Press, Ephrata, PA, 67-100.

Davidson, K. L., G. E. Schacher, C. W. Fairall and A. K. Goroch, 1981: "Verification of the Bulk Method for Calculating Overwater Optical Turbulence", Applied Optics, 20, 2919-2924.

Fairall, C. W., 1980: Estimation of C_n^2 from Bulk Meteorology Data - the NPS Model, BDM Corp. Report BDM/M-009-80, 2600 Garden Rd., Monterey, CA. 7 pp.

Fairall, C. W., K. L. Davidson, G. E. Schacher and T. M. Houlihan, 1978: Evaporation Duct Height Measurements in the Mid-Atlantic, Naval Postgraduate School Technical Report NPS-61-78-005, Monterey, CA. 136 pp.

Friehe, C. A., 1977: "Estimation of the Refractive-Index Temperature Structure Parameter in the Atmospheric Boundary Layer over the Ocean", Applied Optics, 16, 334-340.

Macklin, S. A. and T. H. Guymer, 1980: Inter-platform Comparisons of JASIN WMO Observations, JASIN News No. 15, 5-9.

McPherson, T. R., 1981: Synoptic Classification of Optical Turbulent Regimes, MS Thesis, Naval Postgraduate School, Monterey, CA. 92 pp.

Rosenthal, J., 1976: Refractive Effects Guidebook (REG), Pacific Missile Test Center, Point Mugu, CA, Naval Environmental Prediction Research Facility Report, Monterey, CA. 59 pp.

Royal Society, 1978: Air-Sea Interaction Project, Operational Plans for 1978, London, 225 pp.

Royal Society, 1979: Air-Sea Interaction Project: Summary of the 1978 Field Experiment, London, 139 pp.

Schacher, G. E., K. L. Davidson, D. E. Spiel and C. W. Fairall, 1980: Naval Postgraduate School Shipboard and Aircraft Meteorological Equipment, Naval Postgraduate School Project Report NPS-61-80-017PR, Monterey, CA. 23 pp.

Spiel, D. E., 1981: STREX - A Preliminary Report of Naval Postgraduate School Data. BDM Corp. Technical Report BDM/M-TR-0004-81, 2600 Garden Rd., Monterey, CA. 60 pp.

Wyngaard, J. C., 1973: "On Surface Layer Turbulence", Workshop on Micrometeorology, Amer. Met. Soc. Publication, Science Press, Ephrata, PA, 101-149.

Appendix A

Table Al lists the REG category which applied in the experimental area for individual days of each experiment studied.

Table Al

REG Classification of Individual Experiments

Experiment	Date	REG Profile	Experiment	Date	REG Profile
KANE (1978)	1 Mar	B	CTQ (1979)	2 Jun	B
	2 Mar	B		3 Jun	B
	3 Mar	B		4 Jun	B
	4 Mar	B		5 Jun	B
	5 Mar	J		6 Jun	D
	6 Mar	B		7 Jun	B
	7 Mar	B		8 Jun	B
	8 Mar	B			
	9 Mar	B	ARB (1977)	19 Jul	B
	10 Mar	B		20 Jul	B
	11 Mar	B		21 Jul	B
	12 Mar	B		22 Jul	D
	13 Mar	B		23 Jul	D
	14 Mar	B		24 Jul	D
	15 Mar	B		25 Jul	B
				26 Jul	B
MAGAT (1980)	28 Apr	E			
	29 Apr	E	MABLE (1978)	31 Jul	E
	30 Apr	D		1 Aug	E
	1 May	E		2 Aug	E
	2 May	D		3 Aug	E
	3 May	D		4 Aug	B
	4 May	D		5 Aug	B
	5 May	E		6 Aug	B
	6 May	D		7 Aug	E
	7 May	D		8 Aug	E
	8 May	E		9 Aug	E
	9 May	E		10 Aug	E
				11 Aug	J
CEWCOM-78	14 May	E		12 Aug	J
	15 May	E		13 Aug	D
	18 May	F		14 Aug	B
	19 May	F		15 Aug	B
	20 May	F		16 Aug	B
	21 May	E		17 Aug	B
	22 May	F			
	23 May	F			
	24 May	D			
	25 May	D			

Table A1 Cont'd

Experiment	Date	REG Profile	Experiment	Date	REG Profile
JASIN	13 Jul	D	JASIN (1978)	7 Sep	J
	14 Jul	D		8 Sep	K
	15 Jul	D		9 Sep	D
	16 Jul	D		10 Sep	K
	17 Jul	K		11 Sep	D
	18 Jul	D		12 Sep	J
	19 Jul	K		13 Sep	K
	20 Jul	D		14 Sep	K
	21 Jul	J			
	22 Jul	K	CEWCOM-76	23 Sep	D
	23 Jul	K		24 Sep	D
	24 Jul	K		25 Sep	E
	25 Jul	K		26 Sep	E
	26 Jul	K		27 Sep	E
	27 Jul	K		28 Sep	E
	28 Jul	K		29 Sep	K
	29 Jul	K		30 Sep	K
	30 Jul	D		1 Oct	K
	31 Jul	D		4 Oct	D
	1 Aug	D		5 Oct	E
	2 Aug	D		6 Oct	F
	3 Aug	D		7 Oct	F
	4 Aug	D		8 Oct	F
	5 Aug	K		9 Oct	F
	6 Aug	D		10 Oct	E
	7 Aug	D		11 Oct	E
	8 Aug	D		12 Oct	F
	9 Aug	B			
	17 Aug	D	STREX (1980)	6 Nov	J
	18 Aug	K		7 Nov	K
	19 Aug	K		8 Nov	K
	20 Aug	K		9 Nov	K
	21 Aug	K		10 Nov	K
	22 Aug	D		11 Nov	K
	23 Aug	D		12 Nov	K
	24 Aug	D		13 Nov	D
	25 Aug	D		14 Nov	K
	26 Aug	D		15 Nov	K
	27 Aug	D		16 Nov	K
	28 Aug	D		17 Nov	K
	29 Aug	D		18 Nov	D
	30 Aug	D		19 Nov	K
	31 Aug	D		20 Nov	B
	1 Sep	D		21 Nov	B
	2 Sep	J		22 Nov	K
	3 Sep	K		29 Nov	D
	4 Sep	J		30 Nov	D
	5 Sep	D			
	6 Sep	D			

Table A1 Cont'd

Experiment	Date	REG Profile
STREX (1980)	1 Dec	D
	2 Dec	C
	3 Dec	C
	4 Dec	C
	5 Dec	C
	6 Dec	D
	7 Dec	K
	8 Dec	D
	9 Dec	K
	10 Dec	K
	11 Dec	D
	12 Dec	K
	13 Dec	K

Appendix B

Figures B1-B6 show the mean stability as indicated by Z/L, on an hourly basis, for each REG category studied. Bars indicate standard deviation.
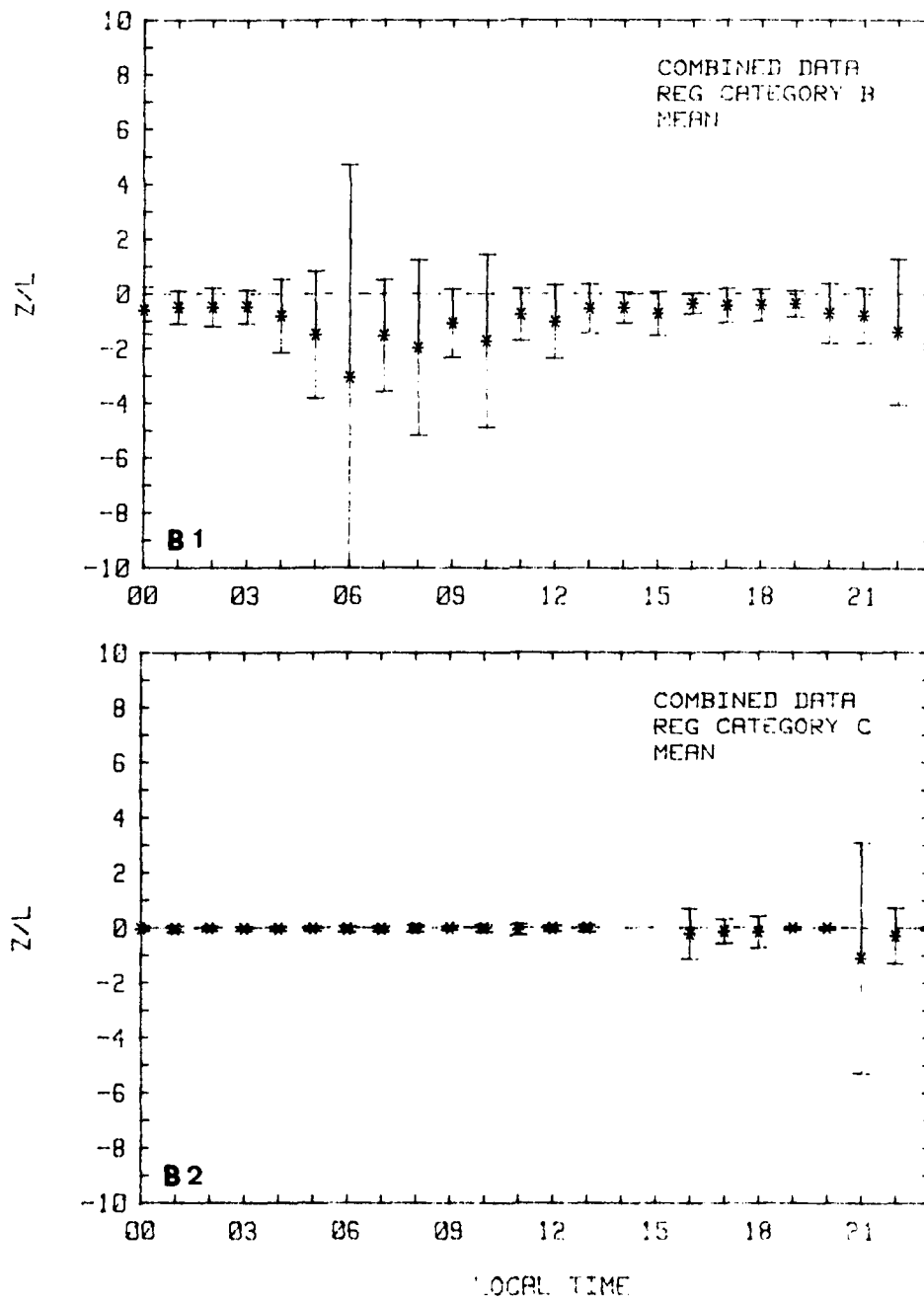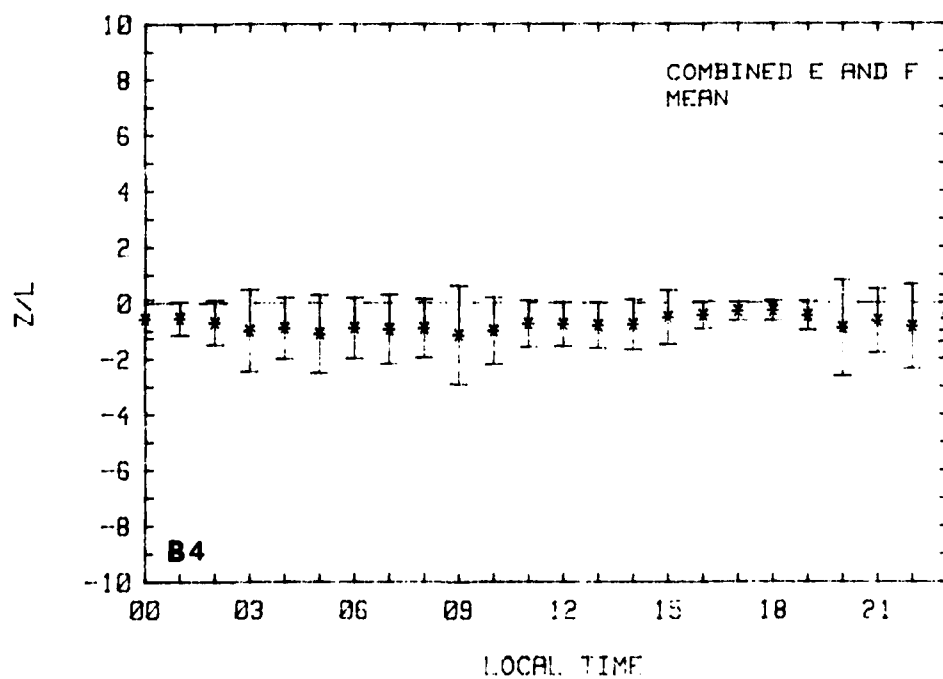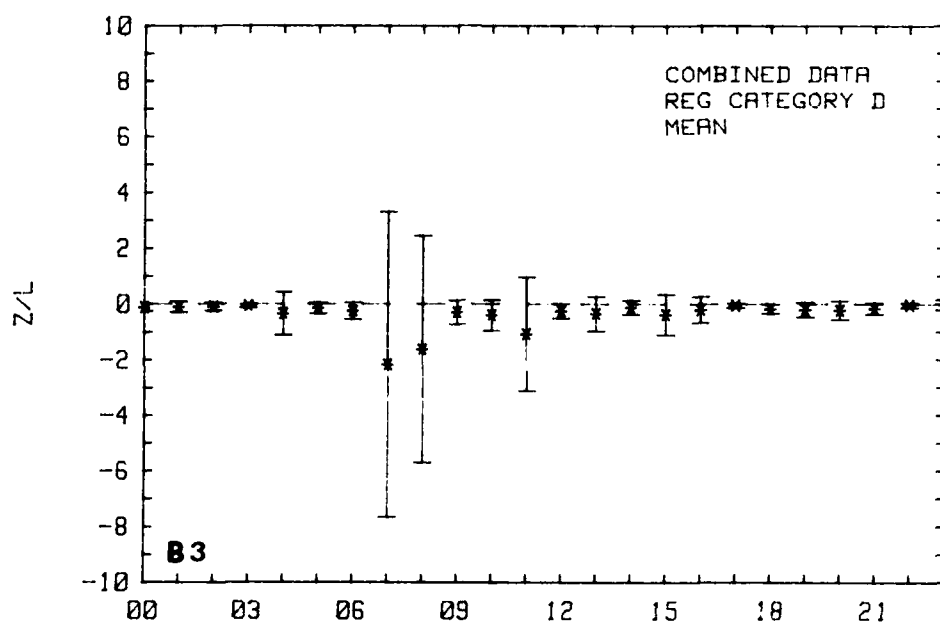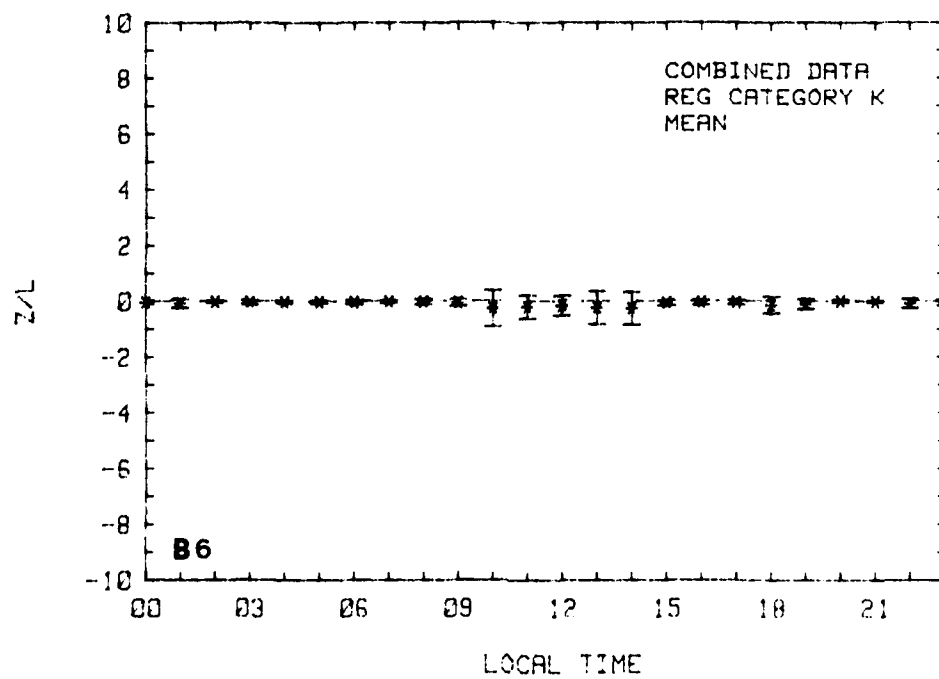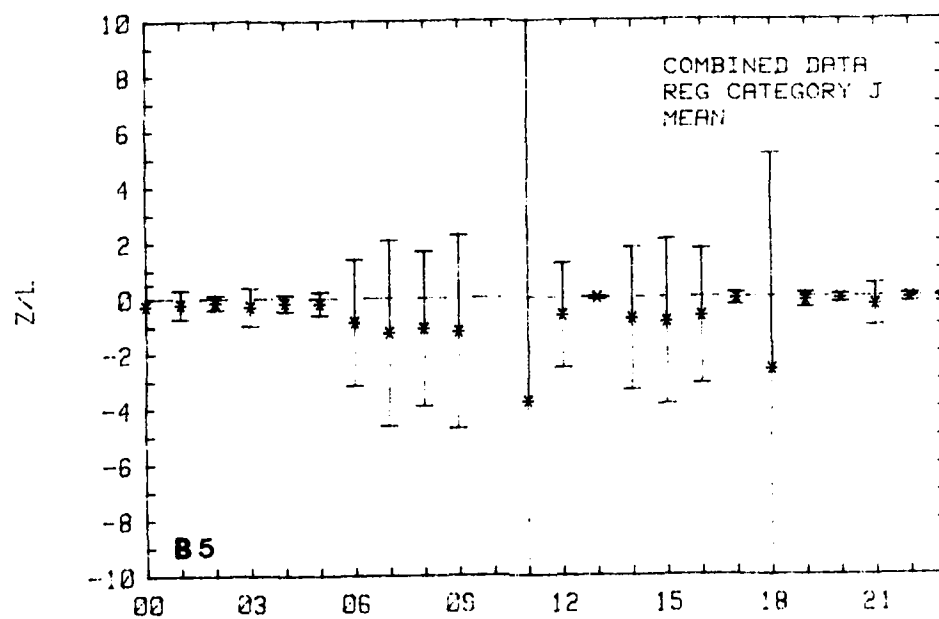
COMBINED DATA
REG CATEGORY B
MEAN

B 1

COMBINED DATA
REG CATEGORY C
MEAN

B 2

LOCAL TIME

COMBINED DATA
REG CATEGORY D
MEAN

B3

COMBINED E AND F
MEAN

B4

LOCAL TIME

COMBINED DATA
REG CATEGORY J
MEAN

B5

COMBINED DATA
REG CATEGORY K
MEAN

B6

LOCAL TIME

Library, Code 0142   4
Naval Postgraduate School
Monterey, California 93943

Office of Research Administration, Code 012   1
Naval Postgraduate School
Monterey, California 93943

Dean of Science and Engineering   1
J. Dyer, Code 06
Naval Postgraduate School
Monterey, California 93943

Professor R.J. Renard, Code 63Rd   1
Naval Postgraduate School
Monterey, California 93943

Professor K.L. Davidson, Code 63Ds   10
Naval Postgraduate School
Monterey, California 93943

Professor G.E. Schacher, Code 61Sq   10
Naval Postgraduate School
Monterey, California 93943

Dr. C.W. Fairall   2
Dept. of Meteorology
Walker Bldg
Penn St. University
University Park, PA   16802

CDR K. Van Sickle   1
Naval Environmental Prediction Research Facility
Monterey, California 93943

Dr. A. Goroch   10
Naval Environmental Prediction Research Facility
Monterey, CA   93943

Dr. Paul Twitchell Code 370C Naval Air Systems Command Washington, D.C. 20360	1
Dr. Barry Katz Code R42 Naval Surface Weapons Center White Oak Laboratory Silver Spring, Maryland 20362	1
Dr. J. H. Richter Code 8320 Naval Research Laboratory Washington, D.C. 20375	1
Dr. Lothar Ruhnke Code 8320 Naval Research Laboratory Washington, D.C. 20375	1
Commander PMS-405 Naval Sea Systems Command Washington, D.C. 20360	1
Dr. Steven Burke Naval Environmental Prediction Research Facility Monterey, CA 93943	1
Mr. Jay Rosenthal Geophysics Division Pacific Missile Range Mt. Mugu, CA 93042	1
Dr. Michael J. Kraus AFGL/LYS Hanscom AFB, MA 01731	1
MAJ Ed Kolczynski AWS/SYX Scott AFB, IL 62225	1

Joel S. Davis   1
Defense Sciences Div.
Science Applications, Inc.
1010 Woodman Dr., Suite 200
Dayton, OH 45432

Mr. L. Biberman   1
Institute for Defense Analysis
400 Army Navy Dr.
Arlington, VA 22202

Mr. Glen Spaulding   1
MAT 72
Naval Material Command
Washington, D.C. 20362

Commander   1
Naval Oceanography Command
NSTL Station, MS 39529

Dr. Ed Monahan   1
Dept of Oceanography
University College
Gallway, IRELAND

Dr. Warren Denner   1
Science Applications, Inc.
2999 Monterey-Salinas Hwy
Monterey, CA 93940

Dr. J.C. Wyngaard   1
CIRES
University of Colorado/NOAA
Boulder, CO 80309

Dr. Marvin L. Wesely   1
Radiological & Environmental Research Division
Argonne National Laboratory
Argonne, IL 60439

Dr. Kristina Katsaros   1
Atmospheric Sciences Dept.
University of Washington
Seattle, WA 98195